CHAPTER 4

THE WEAR OF METALS; THEORY, MECHANISMS AND TESTING.

4.1 Introduction.

Wear is not an exact science, its study incorporates many scientific disciplines and principles whose complex inter-relationships can give rise to considerable areas of uncertainty. Many definitions of wear have been proposed; the following is given in specification DIN 50 320[DIN 1979]:

"Wear is the progressive loss of substance from the surface of a solid body caused by mechanical action, i.e., contact and relative motion with a solid, liquid or gaseous counter-body".

The study of wear, friction and lubrication, as part of the science and technology of inter-acting surfaces, are encompassed by the term *tribology*.

Wear resistance is *not an intrinsic material property*. Many industrialists hope for a wear test equivalent of the hardness or tensile test and it remains difficult for some to understand why this is not possible. Changes to surface and near surface structures during wear contact normally significantly alter local material properties, both mechanically and chemically and, between different wear situations, so many variables apply that direct wear performance comparisons are not possible. However, with controlled laboratory wear tests, specific comparisons can sometimes be made although results often have only a qualified application to the modelled engineering situation.

To form a basis for wear testing one can adopt a "systems approach". That of Czichos[1981] is well known and was used to formulate wear testing specification DIN 50 320[DIN 1979]. This is further described in Section 4.3.

For a given set of conditions, wear behaviour is normally divided into two time based categories, "running-in" and "steady state". During steady state, wear conditions are relatively stable and can be comparatively examined. During running-in, conditions are far more complex and variable, eg., due to work hardening, surface chemistry changes, plastic deformation of asperities, material phase changes etc. Although wear rates are generally higher during running-in, this is not always the case.

4.2 The relationship between wear and friction.

Wear cannot be directly related to friction - this was clearly illustrated by Archard and Hirst[1956; also shown in Archard, 1980] (Table 4.1). Czichos[1974] has shown that friction is just one of several outputs from the general engineering system where wear occurs (Figure 4.1). However, note that this figure does not have heat generation as an output despite this being highly significant. Friction involves the dissipation of some of the energy input into the system[Rigney and Shewmon, 1981]. With metallic contact, a significant energy dissipative process is local plastic deformation. The subsequent generation of wear debris can involve, to varying degrees, micro- and macro-fracture, heat generation and tribochemical reactions, re-working and dispersal of debris and sometimes phase change effects. Therefore one cannot expect any clear correlation between friction and wear.

These next three paragraphs draw from a historical overview of friction and wear by Tabor[1987].

Coulomb had noted that frictional (tangential) force "T" was not quite proportional to normal load "P" and he amended Amonton's Friction Law to $T = \mu P + b$, where μ is the friction coefficient, b is a second smaller term as a result of adhesion, and μP is due to the lifting of asperities over each other; this was derived from the fact that friction was observed to be almost independent of the size of the contacting bodies. However, this old model took no account of the dissapation of energy; viz, the deformation and fracture of asperities and the generation of heat. It can be shown that the average size of asperity contact is constant, irrespective of whether their deformation is elastic, plastic or both, and that, (true area of contact) / (apparent area of contact) = (normal load) / 0.6 (asperity hardness)

Therefore, in contrast to Coulomb's interpretation, adhesion can have a significant role in friction as the true contact area is dependent solely on normal load for both elastic and plastic regimes. For example, a "smooth" copper sphere dry sliding on "smooth" steel generates a friction coefficient of 0.8; here there is adhesive transfer of copper to steel. With a soap lubricant layer of just 0.01μm, transfer is eliminated and $\mu \approx 0.1$. If there is just abrasive contact, where a hard steel sphere "ploughs" a copper surface, with similar lubrication to eliminate adhesion, the value of μ will only increase slightly to between 0.1 and 0.2.

Friction has components of "deformation, adhesion, surface film generation and thermal work dissipation". The friction equation can be re-formulated with friction/tractive force $T = A_t k + C$, where "$A_t k$" is an "adhesion term" (where A_t is true contact area and k a term for shear strength) and "C" an "abrasion term" describing ploughing deformation. The shear strength of many solids can increase with contact pressure, p, thus shear strength term k can be re-written as $k = k_o + \alpha p$, where k_o is bulk shear strength and α is the pressure coefficient of shear strength. Area A_t can be re-written as P/p, where P is the normal force, and therefore T as, $T = (k_o + \alpha p).P/p + C$. The friction coefficient, μ, can then be expressed as,

$$\mu = T/P = k_o/p + \alpha + C/p \tag{4.1}$$

This expression for friction has three terms. For metals the first two terms dominate. For polymers and non-crystalline solids the second term is most important, i.e., $\mu \approx \alpha$. For abrasive contact it is the third term. It can be shown that the significant factor for the coefficient of friction due to (ploughing) abrasion, μ_p, is the effective slope of the asperities, θ. For the elastic sliding of rigid asperities, $\mu_p = \tan\theta$. For a soft surface being ploughed by hard asperities, $\mu_p = (2/\pi)\tan\theta$ for a regular shape and, for a wedge, $\mu_p = \tan\theta$ again.

It will be seen from the results given in Chapter 9 that there is no clear relationship between wear rate and the coefficient of traction; this coefficient was generally higher for low wear rate tests in the mild wear regime. It should be remembered that the degree of surface damage should be related to the magnitude of the tractive force and not just the traction or friction coefficient.

4.3 A systems approach to wear.

The European standards for wear testing, DIN 50 320[1979] and DIN 50 321[1979], have a systems approach. The system is shown in Figure 4.2 and can be analysed as follows:

* *What is the technical purpose of the wear system?*

For example, consider an overview of rail tracked transport systems where the development of linear motors with non-contact vehicle propulsion (magnetic or air-cushion) eliminates the wheel-rail contact problem. Thus the development costs involved in reducing wheel/rail wear and fatigue could be balanced against the cost of developing totally new, non-contact rail systems.

* *Operating variables.*

These can include temperature, time, applied loads, relative velocities and the different kinds of mechanical motion. The last is compared with mechanical actions on materials in Figure 4.3. Welsh's work[1965] on plain carbon steels clearly demonstrated that small changes in operating variables can have a marked effect on wear rate, often by two to three orders of magnitude.

* *The structure of the system.*

As shown in Figure 4.2 this is usually represented by 4 elements (body, counter-body, interfacial medium and environment), the separate properties of those elements and the interactions between them. These interactions can be described by the contact condition, friction condition and by the wear mechanisms that are operative. Exactly what these mechanisms are requires further examination. Wear can be viewed as a function of the system's structure and its operating variables.

4.4 Wear mechanisms and theories.

DIN 50 320 gives four types of general wear mechanism (cf. Table 4.2):

* adhesion
* abrasion
* surface fatigue
* tribochemical reactions.

None of these mechanisms can exist in isolation although one may dominate, particularly the abrasive wear of a soft surface by hard asperities. Even here, material will fracture off the surface by micro-fatigue and, on a microscopic scale, soft material will adhere to the flanks of sliding hard particles.

Other wear processes are often given as specific "mechanisms", for example[Rigney and Shewmon, 1981; Scott, 1979; Hirst, 1965].

* scuffing (the roughening of a lubricated, polished surface).
* fretting (wear from short oscillating motions).
* impact erosion (by solid or liquid particles).
* flow erosion (by liquid or gas).

In general these phenomena can be incorporated within the four DIN mechanisms.

4.5 Adhesive wear

On a microscopic scale, even polished surfaces have a degree of roughness; Archard[1980] drew a visual parallel with gently rolling hills. As a result, between most engineering surfaces, there is only asperity contact with the true contact area being far less than apparent and with initial contact stresses (for the contact of asperities) far higher than apparent.

In vacuum, clean metal surfaces will bond by inter-diffusion / solute action and by inter-atomic (Van de Waal's) forces, with the bond strength normally increasing with pressure, temperature and time. With normal engineering contacts, lubricated in an air environment, surface contaminant such as oxide and surface reactive lubricant additives, prevent such material bonding. If such films are disrupted or transformed then bonding occurs. Initial asperity contact pressures tend to be large enough to generate plastic deformation of asperity crowns with resultant disruption of surface films and subsequent bonding.

Archard[1980] examined the contact mechanics of multiple asperity contacts with respect to their elastic and plastic deformations. He derived a relationship $A_t = P/p_m$, or $A_t = P/H$, where A_t is the true (asperity) contact area, P is the normal applied load and p_m is the mean contact stress, which can also be described by the Brinell hardness H *(at the surface, not bulk)*. Therefore in a single rubbing pass, where two asperities form a circular contact area of maximum radius a, the contact area $\delta A_t = \pi a^2 = \delta P/H$. He made the assumption that adhesive welding of the contact generates a worn particle from the weaker material of volume δV, proportional to the contact area which can be viewed as hemispherical. Therefore $\delta V = 2\pi a^3/3$ for a sliding distance of $\delta L = 2a$ and $\delta V/\delta L = \pi a^2/3 = \delta A_t/3 = \delta P/3H$. To summate for all asperity contacts,

$$V/L = \Sigma(\delta V/\delta L) = (K_1/3).\Sigma(\delta A_t) = (K_1/3).(P/H) = K.(P/H) \qquad (4.2)$$

"K" has been called the (dimensionless) "wear coefficient". In this equation, as constant temperature and thus constant mechanical properties have been assumed, the wear rate is independent of sliding velocity and apparent area of contact. This is because the true area of contact is proportional to the load, therefore K represents the proportion of asperity contacts which generate a wear particle. "1/K" is sometimes described as the "wear resistance".

Table 4.1 shows derived values of K for pin on disc dry sliding tests carried out by Archard and Hirst[1956] on materials with a wide range of hardness values. From these results Hirst[1965] made several general observations on the nature of wear:
* The total range of hardness was $\approx 10^3$, wear rate $\approx 10^5$ and K $\approx 10^5$.
* Wear rates of the hardest (tungsten carbide) and softest materials (bakelite and polythene) were within a factor of 10.
* Whereas the hardness ratio for tungsten and mild steel was $\approx$6:1, the corresponding ratio for K was 7000:1, i.e. K seemed to be a more significant determinant of wear

rate than hardness.

Hirst also commented that, for clean steel surfaces, K will be ≈0.1. However for oxidised steel surfaces sliding in a mild wear regime, and for plastics, it can become as low as 10^{-7}. This reflects the decrease in adhesive wear. Archard's relationship (Equation 4.2, sometimes called "Archard's Law") predicts that wear is proportional to load only where K is constant, whereas in most circumstances an increase in load changes the temperature of the complete wear system with consequent changes in hardness and tribochemical effects.

Rigney and Shewmon[1981] have commented that simple wear laws, like Archard's linear law, are of limited use. They have reviewed the work of Bowden and Tabor[1950, 1964, 1967, 1973] who modelled friction in terms of the shear strength of adhered asperity junctions. If normal load P is supported by total area A_t of asperity junctions, and τ_j is the shear strength of the junctions, then friction force $T = A_t.\tau_j = P/p_m.\tau_j$ where p_m is mean contact stress* (* They have used "po" which is always a symbol for maximum contact stress, but it is assumed here that they mean "pm"). Therefore the coefficient of friction $\mu = \tau_j/p_m$. It must be assumed that this shear strength is that of either the junction or one the bodies, if lower. This formula gives typical μ values (for adhesive wear) of around 0.2 to 0.3. Where surface films reduce the shear strength (τ_i) to that of the contaminated junction, then $\mu \propto (-1 + 1/\kappa^2)^{-1}$ where $\kappa = \tau_i/\tau_{metal}$. Where κ is small, μ is small and as μ rapidly increases as $\kappa \rightarrow 1$. The model also includes a further friction contribution from abrasive ploughing by hard asperities.

Rigney and Shewmon point out that, with different wear systems, wear coefficient K can vary dramatically and that, in addition to hardness, other material variables affect wear rate, eg. temperature, work hardening, fracture toughness, crystallographic changes, chemical reactivity, second phase volumes and distributions, etc. Archard and others have adopted Equation 4.2 to include some other factors, as will be seen in the following sections. However many wear models do not account for the action of debris at the interface. Some investigators have linked adhesive wear to tribo-fatigue, such that $V/L \propto N^{-1}$ where N is the number of cycles to failure (see Section 4.7).

Challen et al[1987] have linked experimental work to Archard's equation (Equ.4.2). They relate K to the coefficient of friction thus, $K \propto \mu^n$ where n is between 4 and 5, thus small changes in μ can be associated with large changes in wear rate. K and μ are related by slipline field theory for asperity deformations, together with a low cycle fatigue model, rather than shear of adhesive junctions. Its significance is that adhesion, and the subsequent transfer of harder material, can then lead to abrasive ploughing of the softer body.

From the results of slow, high contact stress sliding wear tests, Boas and Rosen[1977] postulated that adhesion was a primary wear mechanism. Test specimens were a variety of steels heat-treated to above 400 HV. Their severe wear was found to be independent of strength or ductility. It correlated with microstructural features, particularly carbide size and distribution, and to the strain hardening coefficient.

Rabinowicz[1966] noted that adhesive wear behaviour of pure metals could be related to their ability to form solid solutions, i.e., counterface materials will have higher adhesive wear if they are mutually inter-soluble.

The term *"scuffing"* in engineering wear is often referred to as "adhesive wear", however abrasion and tribochemical actions are also operative. Scuffing is often associated with over-loading during the running-in of lubricated wear couples, where high asperity contact stresses can lead to extensive adhesion before the materials have work hardened and sufficient surface contaminants have been generated (eg., oxide, lubricant additives). Dyson[1979] described the mechanism as one of cumulative damage - initial mild adhesion, more severe adhesion, pitting and finally mild abrasive wear from loose and adhered debris, with corresponding increases in friction and temperature. In such circumstances, the degree of adhesion can be assessed by conductivity measurements, although there is some debate over this experimental method. With severe adhesion, microstructural transformations can occur such as "white etching constituent" (WEC) with steels (a thermomechanically induced, deformed form of martensite, so fine that it remains "white" on etching. WEC is discussed later). Scuffing is of primary concern where initial proving load trials of plant take minimal account of running-in (eg, marine engines).

Although adhesive wear is the predominant mechanism with high friction, dry contact wear such as (non-cooled) pin on disc testing, under such conditions, as contact loads are steadily increased, wear rates can be subject to sudden changes; these are due to thermal and tribochemical effects, rather than any alteration in the adhesion mechanism. This is further discussed in Section 4.9 on dry sliding wear.

During the last ten years, adhesive wear has been studied more on an atomic scale[eg. Pashley, Pethica and Tabor, 1984; Landman et al, 1991, 1992; Sutton, 1994]. Extremely fine pointed styli, as used in atomic probe microscope, have simulated model single asperities in contact with special surfaces (eg. nickel single crystals), in both vacuum and air, i.e., with atomic layers of oxide present. Adhesion has been monitored by electrical resistance measurements. Surface forces alone were found to initiate plastic deformation. Oxide molecular monolayers had little effect but layers >5nm thick greatly affected adhesion. It was found that the plastic yield stress of very small volumes was three to four times greater than bulk values[Pashley et al, 1984]. For elastic solids, asperity adhesion and deformation was expressed in terms of surface energy, elastic modulus and viscoelastic losses. Shearing of such fine adhesive junctions was found to occur in the probe tip rather than at the bond; as the material separated and thinned the atomic disorder was found to approach that of a liquid[Sutton, 1994]. Such work has increased the understanding the frictional force generated by asperity contact and it has been applied in the tribology of electronic microdevices.

4.6 Abrasive wear.

This can be viewed as the removal of material due to the indentation of hard asperities into a softer surface and their subsequent movement. The hard asperities can be the counterface material (2 body wear) or hard debris particles (3 body wear). These "micro-plough" the softer surface(s) pushing a wedge of material ahead and displacing material to each side. With a certain asperity angular shape and with it inclined beyond a certain angle, micro-cutting of the surface can occur, as in any machining operation. In the wake of the asperity, micro-cracks can be generated due to the surface tensile stresses. This is often tribologically termed as "galling".

Tabor[1987] examined how much surface ploughing contributes to friction. Using a simple model (Figure 4.4), which ignores vertical and horizontal material deformations, the ploughing component of friction, μ_p, is described in terms of the force required to displace a surface depression of area A_2, divided by the contact area A_1 (half the static contact area) which would normally support that moving load; both of radius "a". Therefore for a spherical asperity of radius "R",

$$\mu_p = A_2/A_1 = (2a^3/3R)/(\pi a^2/2) = 4a/3\pi R \approx 0.6(t/R)^{1/2} \qquad (4.3)$$

i.e., friction is dependent upon the depth of penetration "t".
For a conical asperity of slope θ,

$$\mu_p = A_2/A_1 = (a^2\tan\theta)/(\pi a^2/2) = (2/\pi)\tan\theta \qquad (4.4)$$

i.e., here friction is independent of penetration depth and solely dependent upon asperity sharpness.

Tabor[1987] further examined friction with respect to both abrasive ploughing and adhesion. Deformation of the softer surface by a hard asperity can be described in terms of slip lines tracing the field where critical shear stress, "k", is reached ("slip-line field theory"). If examined in two dimensions, where the asperity becomes a wedge (Figure 4.5), material displaced from the leading edge (with an assuption of zero adhesion) will become a moving prow ahead of the contact and the wedge quickly lift back to the original surface level, "ironing out" the surface in front (cf. a burnishing process). In this model, wear can only occur from fatigue of the sheared surface layers. It can be shown that, once again, $\mu_p = \tan\theta$, where θ is the angle from the horizontal of both the indentor slope and that of the deformation generated asperity. If θ is too large adhesion will occur and/or the softer asperity will be sheared off. The strength of the bond between the soft and hard asperity can be described in terms of the traction required to produce sliding as a function of shear strength, τ = fk. f = 0 for zero adhesion and pure ploughing and f = 1 for complete seizure. If values of μ, for $\theta = 0$, are seen as the adhesion component of friction μ_a, and for f = 0 as the ploughing component μ_p, then for small values of θ, $<5^o$, and for observed friction coefficients of <0.5, combined friction is near the sum of the two processes, $\mu = \mu_a + \mu_p$, i.e. the two term Coulomb relationship. In engineering practice, slopes $>5^o$ rarely exist and thus μ_p would contribute <0.1 to the total friction. Since for dry metallic contact, $\mu > 0.2$, adhesion must account for at least half of the interfacial friction.

Archard[1980] used a simplified model (Figure 4.6) to analyse abrasion. The hardness of the abrading body is assumed to greatly exceed that of the abraded and there is pure cutting rather than plastic flow (ploughing). A singular abrasive asperity has an idealised shape, a semi-cone of angle ϕ. Under the load contribution of that asperity "δP", the abraded surface is indented to a depth "z" and has an indentation hardness of "H"; the load supporting only the leading half as the contact moves forward. It can then be shown that $\delta P = \frac{1}{2}\pi z^2 \tan_2\phi H$. From geometric assuption, volume removed "δV", per sliding increment δL, is $\delta V = (z^2 \tan\phi)\delta L$. Combining these equations, $\delta V/\delta L = (2\cot\phi/\pi).(\delta P/H)$ therefore,

$$V/L = K_2.(2\cot\phi_{av}/\pi).(P/H) = K.(P/H) \tag{4.5}$$

where K_2 is a constant of proportionality and $\cot\phi_{av}$ is an average value for all the abrasive particles; i.e., here Archard has re-described his basic wear equation (Equation 4.2) and K is highly dependent upon asperity shape.

This simplified view takes no account of the way in which material is removed, of material deformation around the indentor, of strain hardening, of oxide formation nor of hard phase debris abrasion. Abrasion can be viewed as a primary wear mechanism where the wear couple greatly differ in hardness, as for example, with the grinding and polishing of metals, with agricultural equipment and with mineral extraction equipment. If thermal effects during severe wear significantly soften just one body of a wear couple, then the significance of the abrasive mèchanism will be increased.

Khruschov[1974] developed some "principles of abrasive wear" through the study of fixed ceramic grains abrading against pure metals, work-hardened metals, heat-treated steels, wear resistant metals and ceramics. Abrasive wear resistance was correlated with the physical properties of the materials. Some of his conclusions were as follows:

* Steady state wear was proportional to contact stress and sliding distance.
* At low speeds such that there is no significant heating, wear rate was independent of sliding speed.
* Wear rate increased in direct proportion to abrasive grain size up to a limiting size, beyond which there was little effect.
* The dual action of debris clogging the abrasive, and impregnating the abraded, could fundamentally affect wear rate.
* There were limitations to the correlation of wear rate with wear surface hardness. If H_a is the hardness of the abrading grains and H_m that of the abraded material, where $H_a/H_m < 0.7 \rightarrow 1.0$ there was no abrasive wear and other wear mechanisms were more significant. Where $H_a/H_m >$ a certain factor, $1.3 \rightarrow 1.7$ for most tests, then wear became independent of H_a and was dependent upon abrasive type, shape, size and strength.
* For annealed pure metals and steels, the relative wear resistance, w_r, was directly proportional to surface hardness, $w_r = \text{constant}.H_m$, and also, $w_r = \text{constant}.E_m^{1.3}$, where E_m is the abraded material's modulus of elasticity. This did not apply to hardened and tempered steels where, $w_r = w_{r(0)} + \text{constant}.(H_m - H_{m(0)})$, and "(0)" indicates the properties of the material in the annealed state.
* For heterogeneous materials, abrasive wear resistance was proportional to the volume fraction, shape, distribution and hardness of the constituent parts.
* For cold work hardened metals, wear resistance was found to be proportional to the hardness prior to cold working, not the higher cold worked hardness,

where $H_a >> H_{m\ (after\ cold\ work)}$. Where the two hardness values were not that different, the cold worked hardness became significant.

Khruschov explains this final conclusion by commenting that the abrasive action, on a microscale, works the material to its maximum hardening level, more than can be achieved via cold working. Thus the wear resistance reflects the materials resistance to this high degree of deformation compared to the low degree of deformation experienced during the Vickers hardness test. His results have been summarised by Hornbogen[1981] (Figure 4.7).

Moore[1979] made a distinction between the two mechanisms of abrasion, ploughing deformation and micro-cutting. The latter could be related to the material's fracture toughness, rather than its resistance to plastic deformation. Both Moore and Rigney et al[1981] noted that, with ductile materials, the abrasive work was offset by energy dissipation due to plastic deformation within the material. Where a cutting process was prevalent, friction was far lower and the strain hardened zone far narrower than where ploughing and plastic deformation were prevalent. Moore also commented on earlier work by Khruschov on heterogeneous steel structures (Khruschov and Babichev[1958]). He noted that hard, second phase particles only contributed to abrasion resistance where they were significantly larger than the indentation depth of the abrasives. He observed that large carbides would eventually fracture to form hard debris which, in turn, pushed back into the softer phase thus extruding it into the wear path. Vingsbo and Hogmark[1980] found that measuring the specific grooving energy of differeunt materials gave a clearer indication of abrasive wear behaviour than indentation hardness.

Much consideration has been given to the relationship between abrasive wear rates and the distribution of rake angles of the abrasive particles[eg. Rigney and Shewmon, 1981; Moore, 1979; Eyre, 1979; Challen, 1984]. Investigations have shown that a systems approach to such wear must be taken as this relationship varies considerably with different materials and the wear environment system. Typical distributions of rake angles and the respective forms of abrasive action are shown in Figures 4.8[Mulhearns and Samuels, 1962] and 4.9[Eyre, 1979].

Kato[1992] has carried out pin on disc tests within a scanning electron microscope in a study of the micro-mechanisms of abrasive wear between materials of similar hardness. Disc wear, with initial passes was highly sensitive to small changes in angle of the leading edge of the pin with three distinct mechanisms, cutting, wedge formation and ploughing. Under some conditions, with repeated passes, there was a transition from cutting, to wedge, to "shear tongue" formation (side extrusion and adhesive transfer) and finally to ploughing; the latter marked by a lower steady state wear rate and an increase in friction.

As a cautionary note, Rigney and Shewmon[1981] emphasis the danger of extrapolating abrasive wear behaviour to other wear situations; there is a temptation to do this as controlled abrasion tests are relatively simple and inexpensive to perform. For example, a tool steel will have superior abrasion resistance to a ball bearing steel, however its resistance to rolling-sliding wear will be less.

The chance of the abrasive wear mechanism occurring in isolation is rarely possible; at a microscopic level, high temperatures can be generated at the sliding surfaces, thus promoting adhesion and fatigue fracture. Recent work on metal grinding debris[Lu et al, 1992] has shown that frictionally induced melting and subsequent solidification can occur, with the generation of dendritic spheres, 10 to 50μm in size.

4.7 The fatigue wear mechanism and fracture toughness.

Fatigue in wear can be viewed at two levels, rolling contact fatigue spalling of the contacting surface(s), with surface and/or sub-surface crack intiation and, at a microscopic level, the fatigue and fracture of deformed surface aspertities to form wear debris. With well lubricated engineering surfaces (e.g. bearings), rolling contact fatigue due to sub-surface crack initiation occurs together with minimal surface wear, consequently its scientific treatment is often separate from specific wear research. However, as shown by the contact mechanics considerations described in Chapter 3, as surface friction increases, the maximum contact stress at the surface rises and eventually exceeds that of the sub-surface. This can result in combined wear and fatigue at the surface. Sometimes a balance between wear and surface fatigue can be achieved where wear removes initiating fatigùe microcracks before any significant propagation. Rolling contact fatigue studies, using the wear machines described in this thesis, have been carried out by the author[Garnham & Beynon, 1990; Beynon, Garnham & Sawley, 1994], however, in the present work on dry wear, mostly micro-fatigue wear mechanisms were operative. Only under one test condition was the "macro" surface fatigue mechanism, low cycle fatigue, thought operative.

For the micro-fatigue wear mechanism, Archard[1980] re-described wear coefficient "K" in Equ. 4.2 (V/L = K.P/H) such that 1/K = number of cycles to failure. This was an idealised situation as many system effects, e.g. the degree of oxidation, will greatly affect the relationship. Hornbogen[1975] developed a wear model based of linking abrasive wear behaviour with fracture toughness. He made two observations on Archard's wear relationship above:
- Small changes in operating variables can result in sudden, rapid changes in wear rate.
- Where thermal and/or mechanical treatments result in a reduction of fracture toughness, wear resistance can decrease although hardness has been increased.

Hornbogen saw constant "K" as the probability of decohesion of a certain volume of material from the true contact area. This would be related to surface energy (proportional to friction and adhesion forces) and mechanical properties (proportional to the mechanics by which the material is separated from the surface). For pure materials with flat surfaces, these factors could be described by σ_{TH}, the critical stress required to separate atomic bonds and τ_{TH}, the theoretical shear stress for the start of plastic deformation. However, because materials are never defect free and pure planar surfaces are never experienced, properties such as U.T.S. (σ_B), yield stress (σ_Y), work hardening exponent (m), strain to fracture (ε_F) and fracture toughness (K_{Ic}) are relevant and part of constant "K". For most metals, mechanical or phase hardening mechanisms would reduce wear to less than predicted by Archard's equation, i.e., a wear coefficient "K_1" would be effective where $K_1 > K$. Hornbogen related the two by the plastic strain (ε_d) produced during asperity interaction and the critical strain (ε_c) at which crack start to propagate, i.e. $K_1 = K.(\varepsilon_d/\varepsilon_c)$. Where $\varepsilon_c \geq \varepsilon_d$ the material is so ductile that in effect $K_1 \doteq K$ and wear can be assumed to be constant.

To determine these strains, for n asperities, the total area of asperity contacts (of average radius "a") is $n.\pi a^2 = P/H$. Therefore the average asperity radius produced by plastic deformation can be written, $a = (P/\pi nH)^{1/2}$ which must be proportional to strain ε_d, i.e. $\varepsilon_d \leq c_1.(P/H)^{1/2}$, where c_1 is a factor related to surface morpholgy. Note that if n increases with pressure, this strain decreases. A semi-empirical expression is used to decribe the critical strain for crack propagation where, $\varepsilon_c = \delta^*/L$. Here δ^* is the crack opening displacement and L is the effective gauge length. L is related to work hardening by $L = c^2.m^2$, where c^2 is an empirical constant. Denoting Young's Modulus as E and using the Bilby-Swindon model[1965] to relate δ^* to K_{Ic}, wear rate, $\dot{\omega}$, can be written,

$$\dot{\omega} = K_1.P/H = K.\varepsilon_d/\varepsilon_c.P/H = K.(c_1/c_2).(\{P^{1/2}\ m^2\ E\ \sigma_Y\}/\{H^{1/2}\ K_{Ic}^{\ 2}\}).(P/H) \qquad (4.7)$$

This describes the wear rate for the non-ductile situation where $\varepsilon_d > \varepsilon_c$. With reference to his abrasive wear behaviour figure, used by Khruschov (Figure 4.7), the line for pure materials represents $\varepsilon_d = \varepsilon_c$. At this point for the different materials, with a known (i.e. measured at constant load P) wear rate and hardness, the empirical constant factor, (c_1/c_2), can be determined from Equ. 4.7. With reference to Figure 4.7, the linear wear resistance curve of brittle, ceramic type materials is not adequately described by Equ. 4.7; here wear rate is given by,

$$\dot{\omega} = K.(1 + \ln\{\varepsilon_d/\varepsilon_c\}).P/H \qquad (4.8)$$

To summarise Hornbogen's work, there are three ranges of wear behaviour (Figure 4.10);

I - Archard's relationship applies; wear is not affected by fracture toughness which must be high. Sub-critical crack growth is expected (i.e. mechanical, thermal and corrosion fatigue, stress corrosion) in addition to wear by plastic deformation.

II - Wear behaviour is dependent upon critical crack growth; if toughness decreases relatively more than hardness increases, then wear increases in the manner shown for non-pure and non-brittle materials in Figure 4.7.

III - Archard's relationship again applies for brittle materials, the base curve in Figure 4.7.

Factors favouring the transition from Range I to II are increased pressure, increased strain rate, increased angle of impingment (of abrasive) and decreased fracture toughness. Note that in sliding, as opposed to impact wear, impingment angles will be far less and the kind of wear behaviour described in the present work will be near the Range I to II interface.

For hard metals (tool and die steels, cast irons) and ceramics, Zum Gahr[1981] also developed a model linking fracture toughness with abrasive wear resistance. This gives a critical load (P^*_{crit}) where an abrasive particle removes material by micro-spalling rather than ploughing and cutting,

$$P^*_{crit} = (\pi/4.6)^2.(\rho\ K_{Ic}^2 \sin 2x\ /\ 4\mu^2\ H) \qquad (4.9)$$

where K_{Ic} is the fracture toughness, H the wear surface hardness, μ the friction coefficient, 2x the aperture angle of the wear grooves and ρ is the microstructural "mean free path" between parameters such as carbides, microcracks and graphite lamellae. If D is the average distance between particles ($\approx$ abrasive particle size) and ϕ is a factor dependent upon the fraction of particles carrying the load (0.1 for 10%), then the applied surface pressure $P_{crit} = \phi(P^*_{crit}/D^2)$. The abrasive wear rate, $\dot{\omega}_1$, due to spalling ($P > P_{crit}$) is,

$$\dot{\omega}_1 = 12.13(hd/\rho^2).[(P^{1.5}\ \mu\ H^{0.5})/(K_{Ic}^2 \sin 2x)].\log(P/P_{crit}) \qquad (4.10)$$

where h is the average depth of the wear grooves and d the average size of microstructural parameters such as carbides or micro-cracks. The wear rate, $\dot{\omega}_2$, from the "grooving" form of abrasive wear can be described by Rabinowicz's[1966] adaptation of Archard's relationship,

$$\dot{\omega}^2 = P/(c_a \tan x\ H) \tag{4.11}$$

where c_a is a geometric constant for abrasives (π for cones, $2 \rightarrow 4$ for pyramids). Therefore total wear, $\dot{\omega}$, is,

$$\dot{\omega} = \dot{\omega}_1 + c_b.\dot{\omega}_2 \tag{4.12}$$

where c_b is a factor expressing that, for ductile materials, only part of the wear groove is removed as a wear particle, the balance being plastically displaced. (c_b = 1 for total volume removal.) Commenting on Zum Gahr's work, Rigney and Shewmon[1981] state that, for a number of ferrous alloys, if $K_{Ic} > 15\text{-}20$ MPa $m^{1/2}$, abrasive wear resistance depends only slightly on fracture toughness. However, if $K_{Ic} < 10\text{-}15$ MPa $m^{1/2}$, then it depends strongly on fracture toughness.

4.8 Tribichemical wear mechanisms.

This section only examines the inter-action of the wear couple with the near-contact and bulk environments; the effects of added lubricants are not examined. Just as the hardness at the immediate wear surface differs from bulk hardness, so too will the chemical reactivity at the surface of the wear bodies differ from bulk response. Frictional heat can generate such processes as oxidation, steel decarburization, brass dezincification and near surface hydrogen embrittlement. For metallic contact in air, oxidation is a most significant reaction. Oxides have the dual function of forming both a hard boundary lubricant and fracturing to form hard, but friable, wear debris. Whist this debris can be abrasive, it can also act, on a microscopic scale, as a rolling separator between the surfaces, and more importantly, oxide coatings on a molecularly fine scale greatly inhibit adhesive welding of asperities[Sutton, 1994]. The oxides themselves, adhered or separate, are a wear product resulting in metal loss. Air humidity is also a factor in the oxidative wear process, although this has more significance with some ceramics[Perez et al. (1991)] than with metal.

Krause and Schroelkamp[1982] reviewed the effectiveness of different surface analysis techniques (electron spectroscopy for chemical analysis, ESCA; auger electron spectroscopy, AES; secondary ion mass spectroscopy, SIMS) to study how friction forces affect and alter the reaction layers present on metal surfaces in air. They used a twin disc machine to simulate contact, including that typical of wheel-rail. Their example of some typical friction surface layers is shown in Figure 4.11. For materials in general, pressure, temperature and humidity either promote or hinder oxidation via complex interactions. Using steel rollers they found that, with the onset of plastic deformation at the surface, oxide layer thickness / weight increase was 200 times greater than low temperature oxidation of a non-deformed surface. With continual wear contact, oxide flakes were observed to detach from the oxide layer, not from the oxide steel interface. A new layer would immediately begin to form in the resultant pit. In humid atmospheres, iron oxide gels, hydrates and iron hydroxides formed; these were unstable and could quickly de-hydrate to stable iron oxides and it is these that leave the surface as wear debris. X-ray analysis determined that, from the surface, the oxide layer formation was αFe_2O_3 - γFe_2O_3 - Fe_3O_4 - FeO - αFe. A slightly alloyed iron, rather than steel, had a similar order except that the surface layer was FeOOH, not αFe_2O_3. However, their investigations into speeds of oxidative reactions confirmed that metallic wear surfaces re-oxidize immediately after contact and therefore wear surface examination is conditional and cannot reflect the actual layers at the wear interface.

Archard[1980] developed his wear relationship, described so far for the other wear mechanisms, to account for oxidative wear. It was based on asperity contact where a slow growth of a (wear induced) protective film is assumed and this layer remains protective and undamaged until a critical thickness, λ, when it removed by friction. The growth is thermally activated. Following the same basis for multiple asperity contact developed for Equ. 4.2 (maximum asperity contact area πa^2), the total oxidative wear rate can be written,

$$\dot{\omega} = V/L = K_3.\lambda/2a.\Sigma\pi a^2 = [K_3.(\lambda/2a)].A = KA = K.(W/H) \qquad (4.13)$$

K_3 is the proportionality constant for all tribochemical events which produce a wear particle; it will increase with:

* temperature (exponentially).
* chemical reactivity of the environment.
* chemical reactivity of the wear couple for a given environment.

However, the presence of tribochemical wear products generally inhibits metallic wear from abrasion, adhesion and fatigue.

Quinn et al[1984] have studied the oxidative wear of low alloy steel using (non-cooled) pin on disc sliding wear tests. Conditions were "mild" such that no significant oxidation occurred outside the wear contact. They noted that similar mild wear tests in non-oxidizing atmospheres, such as hydrogen, increase wear by at least one order of magnitude. For oxidative wear, load, and thus frictional heat, were correlated with the predominant type of iron oxide that formed. Below 400°C the formation of α-Fe_2O_3 is favoured; between 400 and 600°C, Fe_3O_4 and above 600°C FeO. The static Arrhenius constant of oxidation for these 3 oxides ($kg^2\ m^{-4}\ s^{-1}$) is respectively 1.5×10^6, 3.2×10^{-2} and 1.1×10^5, whereas they calculated tribological values for the Arrhenius constant of 10^{16}, 10^3 and 10^8 respectively from their work. It was observed that minimum wear coincides with the appearance of Fe_3O_4[Childs (1980) reviewing Quinn's work.]. They amended Archard's relationship for wear rate of total asperity contact to read,

$$\dot{\omega} = [\{d.A_p.\exp(-Q_p/RT_c)\}/\{\xi^2.\rho_o^2.f_o^2.V\}].A \qquad (4.14)$$

where d is the distance of a wearing contact at an asperity, A_p is the Arrhenius constant, Q_p is the activation energy for parabolic oxidation, R is the molar gas constant, ρ_o is the density of oxide formed at the real areas of contact, f_o is the fraction of oxide that is oxygen, V is the sliding speed and T_c is assumed to be the temperature at which the asperity oxidizes. T_c is related to the bulk surface temperature, T_s by $T_c = T_s + T_m$ where T_m is the "hot-spot" temperature for sliding contact. ξ is the "critical oxide film thickness" developed during mild wear, in the form of fractured oxide plateaus of between 1 to 4μm thickness. This thickness tended to stay constant, irrespective of (mild wear) load, indicating that there is a critical thickness for oxide as it forms. Heat flow analysis of the contact will be dependent upon each wear system. Quinn found that, between wear rate transitions, oxidative wear rates and general surface temperature (T_s) were proportional to load. Transitions were associated with sudden changes in T_s and with a change in the balance of oxide types found in the wear debris. Recent work by Quinn[1992, 1994], comparing experimental work with theoretical models, has indicated that the activation energies for the tribo-oxidation of different steels are far less than those for static oxidation, with those for severe oxidational wear considerably less than those for mild oxidational wear. Such results were consistent with his view that severe oxidational wear was a mix of severe metallic wear and mild oxidational wear.

Oxidative wear is also significant with lubricated wear conditions. For example, where there is boundary lubrication (i.e. asperity contact), oxide removal and renewal rates become significant with respect to adhesive scuffing failure. Cutiongco et al[1994] have established a contact stress / velocity failure transition diagram for bearing steel, based upon the effect of stress and velocity on asperity "hotspot" or "flash" temperatures, i.e. oxidation rates. Yamamoto[1983], similarly looked at the effect of steel hardness on scuffing resistance with particular reference to oxide film protection. The work-hardening behaviour of the steel, to thus support an oxide film, rather than initial hardness, was found to be significant.

4.9 Wear mechanism comment.

It has been shown that the four mechanisms are operative to some degree in most wear systems; DIN 50 320 (shown in Table 4.2) classifies wear phenomina in this manner. The wear resistance of a particular material, where one mechanism is predominant, cannot be extrapolated to other to situations where other mechanisms predominate; this has been clearly shown by Czichos[1981] (Figure 4.12).

4.10 Fretting

"Fretting" is sometimes described as a wear "mechanism" whereas it is a wear phenomenon associated with small movement (vibratory) oscillations (< 100 μm) of the contacting bodies, often compiled with the entrapment of resultant debris. Oxide formation, consequent volume expansion and debris entrapment can lead to stress concentrations initiating fatigue wear. Wear tends to be highly dependent on this tribochemical mechanism, although all four mechanisms are operative; operating variables will determine their relative significance. Fretting wear damage is seen vibrating bolted surfaces and on wire ropes. Recent work[Vincent et al, 1992] makes a distinction between "fretting wear" (as described above) and "fretting fatigue", where cracks are initiated within, or at the edge of, loaded contacts. These forms of damage can co-exist although their origins are different. Their paper presents an informed overview of the subject.

4.11 Suh's delamination theory of wear.

This was developed by Suh et al[Suh (1973), Jahanmir & Suh (1974), Suh (1977)] as a model for the generation of flake debris by combined adhesion and tribo-fatigue. As discussed in Chapter 3, with normal loaded contact of solid bodies, maximum stresses are sub-surface and, if tangential force is progressively applied (as in sliding) the maximum stress moves towards the surface. At friction levels seen with dry sliding, maximum stress will be at the surface. Within this stressed surface layer, Suh proposes that the material at the immediate surface cold works (i.e. generates dislocations) to a lesser degree than that a few microns sub-surface, as the free surface can accomodate strains. As a consequence, with continued sliding, dislocations pile-up at this finite distance from the surface and eventually their coalescence results in void formation. Such formation is accelerated by material flow around hard particles such as inclusions, second phase areas and precipitates. Further loading cycles promote void propagation and coalescence and the formation of crack parallel to the surface, a few microns deep. At a critical length (with respect to the material), the separating layer will shear and a micro-sheet of material will spall from the surface. Suh adopted Archard's relationship [$V/L = K.(P/H)$] to read $V/L = K_{del}.P$ where wear coefficient K_{del}, for materials "1" and "2", is,

$$K_{del} = b/4\pi.[\{C_1G_1/\tau_1S_1(1-\upsilon_1)\} + \{C_2G_2/\tau_2S_2(1-\upsilon_2)\}] \qquad (4.15)$$

where b is the Burgher's vector, C is a constant dependent upon surface topography, G the shear modulus, τ is friction stress, S is the critical sliding distance for the removal of a complete layer of wear flakes and υ is Poisson's ratio. This differs from the equations for adhesion (Equ. 4.2), abrasion (Equ. 4.5) and micro-fatigue (Equ.s 4.7, 4.8) in that there is no hardness term H, however the hardness term is implicit in some of the terms defining K_{del}.

Theoretical predictions of flake thickness from this theory were less than those observed and Suh et al made further amendments[*several articles* - *Wear* 44, 1977] to account more for plastic deformation, strain accumulation and fracture behaviour. He made the following observations for rolling-sliding wear;
* Normal and tangential loads result in adhesion and abrasive ploughing of the softer surface until there is effectively hard asperity contact on a planar softer surface.
* Cyclic loading induces accumulative plastic shear deformation but such increments of permanent deformation are far less than the degree of reversible deformation per load cycle.
* Near surface delamination cracks initiate with eventual sheet spalling.
* Scanning electron microscopy[Jahanmir and Suh, 1974] of delaminated twin disc contact surfaces has revealed dimpled ductile fracture, indicative of void formation around inclusions; clean steel was found to have higher delamination resistance.
* Surface topography was found to affect running-in but not steady state wear; typical delamination began once one, or both, surfaces were worn to a certain smoothness.
* No simple relationship was established between stacking fault energy (i.e. crystal plasticity) and delamination[Suh and Saka, 1977]; the inter-relationship between tangential force, plastic strain accumulation, crack initiation and crack propagation was too complex.
* Wear rate decreases drastically when shear deformation of the surface is inhibited.
* Adhesive, fretting and fatigue wear are caused by the same mechanisms[Suh, 1973].

Don and Rigney[1985] postulated an alternative theory for flake deformation in that laminates of mechanically mixed, fine "transfer" debris form on the wear surfaces and that these shear off at critical tangential force levels which relate to the laminate thickness. Kaneta et al[1985] have numerically analysed Suh type delàminate cracks and the opening behaviour of their leading and trailing edges. Both were opened during the stress cycle. Circular and elliptical cracks were found to behave similarly. The analysis compared favourably with an experiments on an artificial two dimensional crack. Stress modes were analysed with respect to varying normal and tangential loads.

Hirth and Rigney[1979] found that dislocation microstructures, generated by normal fatigue loading, were similar to those of metals experiencing sliding* friction and wear. (* Low velocity sliding therefore no significant bulk temperature increases.) They determined that any surface soft layers were within 25 to 400 nm of the surface, far smaller than the ≈10μm thickness of sliding flake debris. However they state that a such a layer is not a prerequisite for delamination to occur. They determined an alternative model to Suh's[1977] for delamination (Figure 4.13). In this figure, prospective flake thicknesses, z_a and z_b, are not equal and would depend on substrate properties. They state that cracks propagate parallel to the surface as; (i) the principal plastic shear acts on that plane in the sub-surface region and (ii) cracks will follow dislocation cell boundaries, as indicated by fatigue crack results, and such cells are flattened out sub-surface making more crack paths available in that plane. Some limited experimentation showed that materials with high fatigue resistance, due to easy basal slip and low stacking fault energy, had lower rates.

In the present work, no sub/near-surface crack initiation was observed except along inclusion boundaries; Suh type mechanisms have rarely been observed by this author and then only with lubricated contact.

4.12 Wear by gas and liquid flow.

Erosive, impact and flow wear by liquids or gas on a solid counter-body (e.g. rain erosion of turbine blades) cannot be simply analysed via the four wear mechanisms. A parallel can be drawn with fatigue and creep as damage is cumulative over long time periods with repeated pressure impact and/or high pressure flow.

4.13 Extrusive wear mechanisms.

As discussed above, flake (or "plate" or "tongue") type debris is common with dry sliding and dry rolling-sliding wear of metals. Rather than the delamination of surface strained layers, shallow angled, *surface* initiated, fatigue cracks have been observed to form (by this author) due to plastic ratchetting of the surface structure and eventual ductility exhaustion of the surface layers. Without bulk constraint, material compressed between the angled crack and the surface can be further extruded until it eventually fractures clear, due to low cycle fatigue, in the form of a wear flake. Using slip-line field theory, Olver[1985] has shown that the stress required to cause this extrusion, parallel to the crack face, is very much less than that required for plastic indentation. He has named this process as an "extrusive wear mechanism."

Kapoor and Johnson[1993] have similarly studied the formation of thin flake wear debris. A soft metal wedge sliding on a flat hard metal surface, or vice versa, was used to model single asperity contact under conditions of boundary lubrication. Fine slivers of the softer material were extruded from the contact. They examined this extrusion due to plastic ratchetting and proposed two mechanisms; (i) "working" of the softer surface by hard asperities on the counterbody and (ii) cyclic stressing of the softer surface by the *stress concentrations which occur at the edges* of a hard sliding counterbody. The kinematical shakedown theorem (discussed in Chapter 3) was used to determine the asperity contact pressures required for this mechanism. They determined that the mechanism would still be operative under frictionless conditions. For grooved surfaces, where ridges were aligned with sliding, material was extruded laterally from either side of the ridge; where grooves were normal to sliding, material was extruded longitudinally from the trailing edge of a ridge. Shakedown pressures for frictionless contact were in the range 3.09k to 3.14k (where k is the shear yield stress, for cyclic contact, of the softer material); frictional traction reduces these pressures a little. Hertz contact pressures for initial yield are 2.4k (line contact) and 2.1k (circular contact) with plastic collapse at 5.5k. Extruded flake thickness was of the order of 0.3a to 0.5a, where a is the semi-width of asperity contacts.

A parallel could be drawn with the work described in this thesis where, on a large scale, material was extruded laterally from the edge contact of the cyclindrical discs, above certain contact stress values. However, this edge ratchetting of the discs, and bulk plastic edge distortion, did not correlate with wear rate for the different steels due to microstructural factors. This is further discussed and explained in Chapter 10.

4.14 Dry sliding wear.

The most common type of wear test, because of its simplicity and cheapness, is the pin on disk/cyclinder test where there is pure sliding. Another variation is crossed cylinders. Many wear models have been developed from such studies. The four main wear mechanisms are all relevant and the functions of bulk surface and hot-spot temperatures are crucial. With most steels, for low friction force tests, tribochemical (oxidative) wear is highly significant and, at high friction force, adhesion, abrasion and tribo-fatigue become more significant.

Early research by Welsh[1965], on the (non-cooled) sliding wear of plain carbon steels, was important as he showed that there could be *sudden* transitions in steady state wear rate (Figure 4.14a) with incremental increases in test condition (load, speed etc.). He described the behaviour in the manner of four wear "regimes" separated by three transitions, T_1, T_2 and T_3:-

* $<T_1$ (after running-in). A mild wear regime with a strain hardened surface layer supporting an oxide film; where samples were tempered, or the oxide etched off, a running-in period of severer wear would ensue until conditions were re-established.

* T_1 - T_2. A severe wear regime. Due to increased contact stress and frictional heat, the strain hardened layer can no longer support a continuous oxide film resulting in metal/metal contact and subsequent adhesion and abrasion.

* T_2 - T_3. A second mild wear regime. Further thermomechanical work induces a phase change in the steel; a highly deformed, hard brittle form of martensite is

produced known as "white phase" or "white etching constituent - WEC". (Its structure is so fine that it appears virtually "white"/un-etched with most metallographic examinations.) A sufficient thickness of hard WEC at the surface can once again support a continual oxide film plus resist abrasion and adhesion in its own right.

* $>T_3$. Here the pin (or the small fixed cyclinder in Welsh's work*) and disc (or large moving cylinder*) wear rates usually diverge as the "pin" thermally softens, its WEC tempers back and the oxide layer is lost. The disc stays in the regime above.

The effect of oxygen was shown by repeating the tests in an argon atmosphere. The T_1 - T_2 regime expanded both ways whereas the T_3 transition was not affected. The effects of changing the carbon content of the steel, and thus its hardness and capability to form hard phases, is shown in Figure 4.14b[after Eyre, 1978]. This figure can be interpreted as showing that for mild wear with oxide support, a hardness level of 340 - 425 HV is required, and for mild wear without oxide support a hardness level of 553 - 775 HV is required.

Welsh calculated various "flash-point" or "hot-spot" temperatures (θ_m above the general surface temperature) based on Archard's assumption that a single asperity can momentarily take the full load. The results were related to carbon content, bulk hardness, sliding speed and transition point (T_1, T_2 etc.); these are shown in Table 4.3. θ_m is proportional to the friction coeffcient μ. (Welsh noted that errors may arise from using bulk hardness as the wear surfaces can work harden, phase change harden and thermally soften.) For severe conditions, flash-point temperatures were well above the eutectoid temperatures of the steels ($\approx 725^{\circ}C$).

In a review of dry sliding wear research, Childs[1980] noted that Quinn had disagreed with Welsh on "flash-point" temperatures, estimating them to fall between 250 and 650°C. Childs divides sliding wear behaviour into three mechanical regimes (I, elastic surface stressing; II - plastic burnishing; III - plastic roughening) whose limits depend upon (τ/k), the ratio of interfacial shear strength at an asperity contact to the shear flow stress of the softest material, and on asperity shape. The relationship is shown in Figure 4.15. τ can be influenced by oxide formation and/or by any form of lubrication. k is influenced by strain hardening, thermal softening and the thermomechanical generation of hard phases. Wear rate and running-in behaviour can be based upon the formation and stability of surface films and the near surface layers which support them. Childs discussed Suh's delamination work where sliding was carried out below the T_1 transition with an argon atmosphere to eliminate oxidative wear and protection. Whereas in air, debris was an agglomoration of transfer products from adhesion and oxidation with surface roughening and increasing stress during running-in, in argon, delamination and tribo-fatigue occurred, with surface smoothing and decreasing stress during running-in. Flake debris, 1 to 10μm thick and 10μm² in area, was produced; far smaller than seen with severe wear. Surface roughening in air was thought due to the fact that oxidation resulted in only "patchy" adhesion.

This sliding wear work focussed attention on the "white etching constituent" (WEC). This had been observed on the running-surface of rails (revealed by etching the burnished contact strip). Eyre[1982], in a review of the dry sliding wear of pearlitic steels, thought that this could only occur on rails if there more more slip/creepage than supposed. With his pin on disc tests, he generated WEC in 0.35%C steel pins but it did not form with 0.1%C steel pins. Rowntree[1982] has researched WEC formation. He found it to be an ultrafine form of martensite; too fine for optical microscopic resolution hence the "white" appearance. For plain carbon steels, he calculated that, for a single rubbing pass, temperatures in excess of 1100°C and probably around 1250°C would be required to austenitize lamellar pearlite. For multiple passes, 910°C + would be required for specific "flashpoint" time durations to effect the phase change. Carbon diffusion within austenite is the rate determining factor (cf. Eyre's results above). To summarise, WEC will form in medium to high carbon steels where the summation of asperity interactions results in the requisite "mean flash temperatures"[as determined by Archard, 1980] for the duration of the contact. Hornbogen[1981] similarly determined that WEC was martensitic. He drew a comparison with austenitic manganese steels where transformation to martensite induced by deformation gave a far harder matrix than martensite formed by heat-treatment. He suggested that the reason was that below 200°C carbon atoms segregate to the additional dislocations generated by deformation. He noted that, although hard WEC initially reduces wear, this brittle phase can easily fracture and the resultant debris is highly abrasive.

In contrast to this work, Clayton[1980] examined the dry sliding wear of pearlitic rail steels using *air-cooled* pin on disc tests, as wheel-rail contact is air-cooled. He makes no mention of WEC formation on the pins.

Lim and Ashby[1987] attempted to summarise the mass of dry sliding wear (pin on disc) results that emerged over four decades by developing "wear mechanism maps". Cooled tests were *not* included and heat generation and heat flow were determinates of the wear rate contours. The map shows the normalised wear rate contours of a steel sliding pair on coordinates of normalised contact pressure and normalised sliding velocity. The wear rate under each wear mechanism was determined as a function of thermal, mechanical and chemical properties. Most wear mechanism factors, as described in this chapter, plus some other factors, were taken into account. Wear rate (m^3/m) was normalised by dividing by the apparent contact area, contact pressure by dividing by (room temperature) hardness and sliding velocity by dividing by the thermal diffusivity (i.e. "heat flow velocity"). The result is shown in Figure 4.16.

Welsh's work has recently be re-assessed by Venkatesan and Rigney[1992], using similar crossed cylinder tests in air and vaccum, and the results have been matched against Lim and Ashby's map. The results in air were consistent with this previous work. Even with tests in vacuum, some oxidative debris was found. For comparative tests, surface microstructures in vacuum had clearly ratchetted, whereas they had not in air. The coefficient of friction for steady state mild wear (in air) was around 0.2-0.3; for severe wear the average was similar but with large fluctuations, up to 1.2 in air and 1.8 in vacuum, thus suggesting a high degree of adhesive wear.

4.15 Rolling-sliding wear.

For most rolling bodies, sphere on sphere or sphere on planar, elastic and geometric constraints introduce an element of sliding or creepage, as described in the previous chapter. Additionally, tractive force will generate an additional element of creepage/sliding. The contact mechanics considerations of rolling-sliding contact, as against pure sliding, were described in the previous chapter. Most rolling-sliding tests have been carried out under oil lubricated conditions for the simulation of mechanical couplings, particularly for the automotive and aerospace industries. Under such conditions, wear is mild and failure by rolling contact fatigue is the major consideration. Many test machines use, or simulate, ball bearing contacts. Friction coefficients are typically less than 0.1. Where controlled sliding is required, twin disc machines are usually used, some with twin cylindrical discs, others with one, or both, discs radiussed or chamfered to give the requisite high contact stresses.

The railway wheel-rail contact is unusual in that the contact is normally, nominally unlubricated. Many decades back, the Amsler rolling-sliding (twin disc) wear test machine was developed for the railway industry[Amsler, 1922] and this machine, or a clone, remain a major source of railway industry laboratory wear performance data. With this machine, sliding is induced by a geared 10% rotational speed differential between the discs; further creepage variations are achieved by varying the respective disc radii. The machine is described in detail in Chapter 6. British Rail Research have carried out various Amsler tests. To simulate track debris fall-off with their early work[Beagley, 1976], debris clearance by wire brush was used. These tests showed that with dry contact, as creepage increased, the friction coefficient rose to a limiting value of around 0.6, irrespective of contact stress (Figure 4.17). As with Welsh's work, wear behaviour for the majority of steels examined has been grouped into three regimes, "mild, severe and catastrophic"[Bolton and Clayton, 1984], although, unlike uncooled, pure sliding wear tests, there were no sharp transitions between regimes.

The mild regime, after running-in, was primarily oxidative. Wear was caused by abrasion of the oxide layer, re-oxidation of new material and delamination of surface layers over many cycles due to flattened MnS inclusions developing into surface cracks. As MnS levels and oxidation rates of the steels tested were similar, mild wear rates were similar.

Severe wear was characterised by prominent metallic flake formation after a short running-in period and a rough, metallic wear track appearance.

Catastrophic wear was associated with high adhesion resulting in a very rough wear surface, characterised by "shear micro-pits" where material had been "scooped" from the track.

Nearly all the tests described in this thesis would fit into their mild and severe categories, although some catastrophic behaviour was observed. The severe wear results described by Bolton and Clayton could be defined by a linear relationship, analagous to variations of Archard's Equation described in this chapter. Regime transitions were affected by both creepage and contact stress. Such British rail wear tests, and tests from other rail reseachers, will be considered further in the discussion (Chapter 10).

All the wear mechanisms described so far in this chapter are operative with dry rolling-sliding tests. There are crucial differences between this type of test and pin on disc tests. High contact stresses, representative of wheel/rail contact, are not possible with pin on disc tests due to thermal overload and collapse of the pin. With rolling-sliding tests, short, periodic contact cycles are seen by material elements of both wear tracks; the time out of contact allows for elastic, thermal and some microstructural recovery, plus chemical stabilisation. Such tests can have contact stresses an order of magnitude higher than those for pin on disc, percentage degrees of sliding an order of magnitude lower. Perez-Unzueta[1992] has compared pin/disc sliding tests and rolling-sliding tests in assessing the wear of pearlitic rail steels. Both methods gave similar material rankings. Results from the present work, and those of Clayton et al[1987], indicate that this would not be the case if the four types of bainitic steel were compared with pearlitic rail steels by these two methods. Pin on disc tests remain highly relevant for quick, inexpensive assessments of similar materials; for example, Clayton's[1980] assessment of pearlitic rail steels with respect to small microstructural differences.

4.16 Wear of "composite" structures.

Apart from standard composite materials, many other materials including most forms of steel, have structures which contain hard and soft phases; material bulk hardness values reflect the resistance of the structural mix to (indentation) deformation. In some respects, pearlite is more akin to conventional composites in that the hard cementite phase is lamellar. Its unusually high sliding and rolling-sliding wear resistance, for its bulk hardness value, is based upon this structural difference as will be discussed later in this work. The examination of the effect on wear of hard, second phases, with respect to composition, quantity, shape, orientation and distribution, has mostly been concentrated on tool steels, hot working dies, etc., not low carbon, low alloy steels.

Hornbogen[1981] theoretically examined the effect on wear of a uniform distribution of hard second phase particles, as represented in Figure 4.18. Wear rate was described thus,

$$1/\dot{\omega} = 1/\dot{\omega}_m + (\Delta A_p/A).(1/\dot{\omega}_p - 1/\dot{\omega}_m) \qquad (4.16)$$

where $\dot{\omega}_p$ and $\dot{\omega}_m$ are the respective wear rates for the hard phase and matrix and $(\Delta A_p/A)$ is an expression relating to the proportion of hard particle contact area compared to total contact area. This was assumed to remain constant during wear, although this is often not the case. Figure 4.18 shows the situation with 1% volume of hard phase in a 100:10:1 orientation; i.e., near lamellar. $\Delta A_p/A$ would then be 0.4, 0.04 and 0.004 respective to orientation. The advantage of aligned lamellar hard phase can be seen, however Hornbogen noted that weak cohesion of the hard phase could initiate delamination and consequent abrasive wear due to hard phase particles (cf. Section 4.6).

This simplified model does not account for the strengthening effect of the hard phase on the matrix of the softer phase; dislocation pile-ups, etc.

4.17 Test equipment - a summary overview.

For each wear (system) problem, simulated service test equipment can be constructed, however this usually proves time consuming, expensive and only of localised interest and relevance. Smaller scale laboratory tests can often give rapid, inexpensive indications of material behaviour and results from several sources can be compared. For example, some abrasive tests on metals, using abrasive ceramics counterbodies, have a semi-industrial standardisation to give material rankings for this specific application, but such data cannot be extrapolated to other wear systems.

There are no absolute wear parameters involving standardised test equipment as in materials tests like the Vickers hardness test. The most common wear test procedure is the pin, or ball, on disc test. In Europe, VAMAS have been investigating how to standardise such tests[Almond and Gee, 1987] by comparing test results of similar wear couples, tested under nominally identical contact stress and sliding conditions, from a number of test facilities worldwide (including 10 in the UK). The results appeared to confirm that wear must be system based, part of which includes test machine characteristics (vibrations, heat flow, etc.). The use of chamfered pins, radiussed pins or balls in such sliding tests eliminates pin cutting and "chattering", but contact stress diminishes as the radius wears and contact area increases, thus heat generation and flow are also altered. However steady state results from such tests can be of value where the contact stress change is low; also of value are single rubbing pass tests using radiussed pins or balls.

Many types of rolling contact test machines have been built, but nearly all are exclusively designed for the determination of oil lubricated rolling contact fatigue behaviour. Few machines are suitable for dry rolling-sliding contact tests. The Amsler machine was designed as a general wear test machine; pure rolling, pure sliding or rolling-sliding can be carried out under steady state, cyclic or oscillating test conditions. It has primarily been used by the railway industry for dry rolling-sliding tests. This machine is limited by its geared disc drives which cannot account for the effect of disc wear on contact geometry, stress and creepage. Many adaptations have been made to the machine, or its basics have been used in the design of improved machines (as described in the present work), in order to overcome some of these limitations.

Recent tribological studies[Landman et al, 1992] have been at microscopic level involving the movement of (atomic force microscope) material tips, of just a few molecules in width, moving over a second planar body. Friction and wear mechanisms at this scale have been extrapolated to the performance of asperity interactions.

4.18 Summary.

The investigation and resolution of a wear problem is often complex and requires a systematic, analytical approach of the type specified in DIN 50 320[DIN, 1979]. Within this approach, careful cross-references can be made between different wear situations. Wear cannot be directly related to the coefficient of friction or traction; these are part of the dissipation of the energy input into the system. In this work, there has been an attempt to translate many of the wear system variables operative on rail track on to the operation of small scale laboratory test machines.

The process of wear can be analysed in terms of four mechanisms; adhesion, abrasion, tribo-fatigue / fracture toughness and tribo-chemical reactions. In most engineering wear situations, all four are operative to some degree. This is the case with the wear of rails and similarly with the twin disc tests described in this work. Recent research has examined such mechanisms on a molecular scale.

Within a wear system, with fixed conditions, initial variations in both wear rate and friction are observed as the contacting surfaces "run-in" until stabilised contact conditions, surface finishes and surface material properties are established. In most cases, a period of steady state wear (with respect to time) is then obeserved. Measures which affect running-in can also affect steady state wear rates. Eyre[1979] gives an example where a protective layer of ion implantation into a wear surface resulted in improved steady state wear resistance long after the layer had been worn away.

It has been shown, for both pure sliding and rolling-sliding tests, that as a test variable is incrementally increased or decreased, there can be rapid transitions from one steady state wear rate to another. Should the wear system conditions be around a transition point, oscillations in steady state wear rates can occur. These have been seen in some of the tests described in this work.

Finally, it should be understood that wear rates are determined by material conditions at, and within a few microns of, the contact. For different materials, these may alter in different ways such that ranking by mechanical properties will not be reflected in the respective wear rates. Metals will work harden and shakedown; structures can be significantly changed. For example, wear face traction can alter a matrix from a geometrically homogenous mix of hard and soft phases to an inhomogenous one, akin to a composite structure, therefore, the proportional area of hard phase *in the plane of the contact* must be considered.

In this chapter, a general overview of wear has been given. In the following chapter, the specific wear and fatigue problems of the railway rail are reviewed.

4.19 References.

Almond, E.A. and Gee, M.G. (1987). "Results from a U.K. interlaboratory project on dry sliding wear." *Wear* 120 pp 101-116.

Amsler, A.J. (1922). "Abnützungsmaschine für Metalle (Wear machine for metal)." *Z. VDI*, 66 pp.377-378.

Archard, J.F. and Hirst (1956), *W. Proc. Royal Soc.*, 236 [A], p. 397.

Archard J.F. (1980) "Wear theory and Mechanisms." *Wear Control Handbook*. Pub. ASME; eds. M.B. Peterson and W.O. Winter.

Beagley, T.M. (1976). "Severe wear of rolling-sliding contacts". *Wear* 36 pp. 317-335.

Beynon, J.H., Garnham, J.E. and Sawley, K.S. (1994). "Rolling contact fatigue of four pearlitic rail steels." Initially submitted to *Wear*, August 1994. Re-submitted following review, June 1995.

Bilby, B.A. and Swinton, K.H. (1965). *Proc. Royal Soc.* A285, p. 22.

Boas, M and Rosen, A. (1977). "Effect of load on adhesive wear of steel". *Wear* 44, pp. 213-222.

Bolton, B.J. and Clayton, P. (1984). "Rolling-sliding wear damage in rail and tyre steels". *Wear* 93 pp. 145-165.

Bowden, F.P. and Tabor, D. (1950). *The Friction and Lubrication of Solids, I.* Oxford University Press.

Bowden, F.P. and Tabor, D. (1964). *The Friction and Lubrication of Solids, II.* Oxford University Press.

Bowden, F.P. and Tabor D. (1967). *Friction and Lubrication.* Methuen & Co., Ltd., London.

Bowden, F.P. and Tabor, D. (1973). *Friction: An Introduction to Tribology.* Anchor Press (The Science Study Series).

Challen, J.M. and Oxley, P.L.B. (1984). "The influence of asperity angle and lubrication on friction and wear". *Proc. 11th Leeds-Lyon Symposium on Tribology - "Mixed lubrication and lubricated wear", 1984.* Pub. Butterworths, 1985.

Challen, J.M. Kopalinsky, E.M. and Oxley, P.L.B. (1987). "An asperity deformation model for relating the coefficients of friction and wear in sliding metallic friction". *Proc. Int. Conf. "Tribology - 50 years on"*, at I.Mech.Engrs., London, 1-3/7/1987, *Proc.Inst.Mech.Engrs.* C156, pp. 957-964.

Childs, T.H.C. (1980). "The sliding wear mechanisms of metals, mainly steels." *Trib. Int.* (Dec. 1980), pp. 285-293.

Clayton, P. (1980). "The relationship between wear behaviour and basic material properties for pearlitic steels". *Wear* 60, pp. 75-93.

Clayton, P., Sawley, K.J., Bolton, P.J. and Pell, G.M. (1987). "Wear behaviour of bainitic steels." WEAR 120 pp. 199-220.

Cutiongco, E.C. and Chung, Y-W. (1994). "Prediction of scuffing failure based upon the competitive kinetics of oxide formation and removal: Application to lubricated sliding of AISI 52100 steel on steel." *Trib. Trans.* 37 (3), pp. 622-628.

Czichos, H. (1974). "Failure criteria in thin film lubrication - the concept of a failure surface." Trib. Int. 7 pp. 14-20.

Czichos, H. (1981). "Systems analysis and description of wear processes". *Metallurical Aspects of Wear*, pub. Deutsche Gesellshaft für Metallkunde, pp. 9-22.

DIN 50-320 (1979). "Wear: Systematic analysis of wear processes. Classification of wear phenomina". Pub., Beuth Verlag, Berlin30 and Köln 1, Dec. '79.

DIN 50-321(1979). "Verschleiß-Meßgrößen (Wear-quantities)", ibid.

Don, J. and Rigney, D.A. (1985). "Predictions of debris flake thickness". *Proc. Int. Conf. on "Wear of Materials", Vancouver, Canada, 14-18/4/85*. Pub. ASME.

Dyson, A. (1979). "Scuffing". *Treatise on Materials Science and Technology* 13 ("Wear"), ed. D. Scott, pub. Academic Press (N.York and London), pp. 176-216.

Eyre, T.S. (1979). "Wear resistance of metals." *Treatise on Materials Science and Technology, Vol.13 "Wear"*, pp. 363-442, Ed. D.Scott, pub. Academic Press (New York and London), 1979.

Eyre, T.S. (1982). "Wear of pearlitic steels". *Proc. 2nd. Heavy Haul Rly. Conf., Colorado Springs, U.S.A., 25-29/9/1982*, pp. 277-281.

Garnham, J.E. and Beynon, J.H. (1991). "The early detection of rolling-sliding contact fatigue cracks". *Proc. 3rd. Int. Conf. on "Contact mechanics and wear of rail/wheel systems", Univ. of Cambridge, UK, 22-26/7/1990*. Pub. *Wear* 144 pp. 103-116.

Hirst, W. (1965). "Wear". *Metallurgical Reviews*, 10 (38), pp. 145-172.

Hirth, J.P. and Rigney,D.A. (1979). "Microstructural models for friction and wear." *Proc. 5th Int. Conf. on "Strength of Metals and Alloys", Aachen, Germany, 27-31/8/1979.* Pub. Pergamon (1980), ed. P Haasen et al., Vol.3 of 3.

Hornbogen, E. (1975). "The role of fracture toughness in the wear of metals". *Wear* 33, pp. 251-259.

Hornbogen, E. (1981). "Microstructure and wear". *Metallurgical aspects of wear.* Pub. Deutsche Gesellschaft für Metallkunde, pp. 23-50.

Jahanmir, S. and Suh, N.P. (1974). "Microscopic examination of wear sheet formation by delamination." *Wear* 28, pp. 235-249.

Kaneta, M., Murakami, Y. and Okazaki, T. (1985). "Mechanism of opening / closing of subsurface cracks due to a moving Hertzian loading." *Proc. 12th Leeds-Lyon Symp. on Trib., Lyon, France, 3-6/9/85.* Pub. "Mechanisms of surface distress", Butterworths, ed. Dowson et al.

Kapoor, A. and Johnson, K.L. (1993). Plastic ratchetting as a mechanism of metallic wear. *Cambridge University (UK) Eng. Dept. Report CUED/C-mech/TR55 Aug 93.*

Kato, K. (1992). "Micro-mechanisms of wear - wear modes." *Wear* 153 pp. 277-295.

Khruschov M.M. and Babichev, M.A. (1958). "Resistance to abrasive wear of structurally inhomogeneous materials". *Friction and Wear of Machinery* 12, pp. 5-23.

Khruschov, M.M. (1974). "Principles of abrasive wear". *Wear* 28, pp. 69-88.

Landman, U., Luedtke, W.D. and Ringer, E.M. (1991). "Atomic scale mechanisms of adhesion, friction and wear". *Wear particles: From the cradle to the grave. Proc. 18th Leeds-Lyon Symp. on Tribology, 3-6/9/1991*, ed. D. Dowson et al, pub. Elsevier (1992),pp. 3-25.

Landman, U, Luedtke, W.D. and Ringer, E.M. (1992). "Atomistic mechanisms of adhesive contact formation and interfacial processes." *Wear* 153 pp. 3-30.

Lim, S.C. and Ashby, M.F (1987). "Wear-mechanism maps. (Overview No. 55.)". *Acta metall.* 35 (1) pp. 1-24.

Lu, L., Farris, T.N. and Chandrasekar, S. (1991). "Sliding micro-indentation wear particles: spheres in grinding swarf". *Wear particles: From the cradle to the grave. Proc. 18th Leeds-Lyon Symp. on Tribology, 3-6/9/1991*, ed. D. Dowson et al, pub. Elsevier (1992), pp.257-263.

Moore, M.A. (1979). "Abrasive wear". *Treatise on Materials Science and Technology* 13 ("Wear"), ed. D Scott, pub. Academic Press, (N. York & London), pp. 217-258.

Olver, A.V., (1985). "Extrusion - a new wear mechanism." *Proc. 12th Leeds-Lyon Symp. on Tribology, Lyon, France, 3-6/9/85*. Pub. Butterworths (1985).

Pashley, M.D., Pethica, J.B. and Tabor, D. (1984). "Adhesion and micro-echanical properties of metal surfaces". *Wear* 100, pp. 7-31.

Perez-Unzueta, A.J., Beynon, J.H. and Gee, M.G. (1991). "The effects of surrounding atmosphere on the wear of sintered alumina." *Wear* 146, pp. 176-196.

Perez-Unzueta, A.J. (1992). "Wear resistance of pearlitic rail steels". PhD Thesis, University of Leicester (U.K.).

Quinn, T.F.J., Sullivan, J.L. and Rowson, D.M. (1984). "Origins and development of oxidational wear at low ambient temperatures." *Wear* 94, pp. 175-191.

Quinn, T.F.J., (1992). "Oxidational wear modelling: I." *Wear* 153 pp. 179-200.

Quinn, T.F.J., (1994). "Computational methods applied to oxidative wear". *Presentation to a seminar on "Theoretical and computational methods in friction, lubrication and wear" for the Tribology Group of the Inst. of Physics, 11-5-1994*, Dept. Chem Eng., Imperial College, Univ. of London.

Rabinowicz, E. (1966). *Friction and Wear of Materials*. Pub. John Wiley (London).

Rigney, D.A. and Shewmon, P.G. (1981). "Wear and erosion of metals". *Metallurgical treatises presented at the USA - China Bilateral Conf., Beijing, China, 13-22/11/1981*. Pub. AIME Met. Soc.

Scott, D. (ed.) (1979). *Treatise on materials science and technology* 13 ("Wear"), pub. Academic Press (N.York & London).

Suh, N.P. (1973). "The delamination theory of wear." *Wear* 25, pp. 111-124.

Suh, N.P. (1977). "An overview of the delamination theory of wear." *Wear* 44, pp. 1-16.

Suh, N.P. and Saka, N. (1977). "The stacking fault energy and delamination wear of single phase F.C.C. metals." *Wear* 44, pp. 135-136.

Sutton, A.P. (University of Oxford, UK) (1994). "Modelling adhesion, friction and boundary lubrication". *Presentation to a seminar on "Theoretical and computational methods in friction, lubrication and wear" for the Tribology Group of the Inst. of Physics, 11-5-1994*, Dept. Chem Eng., Imperial College, Univ. of London.

Tabor, D. (1987). "Friction and wear - Developments over the last fifty years." Proc. Int. Conf. "Tribology - 50 years on", 1-3/7/87, I.Mech.E., London. Pub. Proc. Inst. Mech. Engrs. C245, pp. 157-172.

Venkatesan, S. and Rigney, D.A. (1992). "Sliding friction and wear of plain carbon steels in air and vacuum." *Wear* 153 pp. 163-178.

Vincent, L., Berthier, Y., Dubourg, M.C. and Godet, M (1992). "Mechanics and materials in fretting". *Wear* 153 pp. 135-148.

Vingsbo, O. and Hogmark, S. (1980). "Wear of steels". *Proc. ASM materials science seminar on "Fundamentals of friction and wear in materials", 4-5/10/1980, Pittsburgh, Penn., USA*, pub. ASM, ed., D.A. Rigney.

Welsh, N.C. (1965). "The dry wear of steels (Parts I & II)". *Phil. Trans. Royal Soc.* 257 (A1077), pp. 31-70.

Yamamoto, Y. (1983). "The effect of surface hardness of carbon steels on scuffing resistance in rolling-sliding contact." *Wear* 89, pp. 225-234.

Zum Gahr, K.H. (1981). "Abrasive wear of metallic materials." Metallurgical aspects of wear. Pub. Deutsche Gesellschaft für Metallkunde, pp. 73-104.

Pin material*	Wear rate 10^{-10} cm^3/cm	Hardness# (bulk) HV	Coeff. friction μ	Archard's wear coeff. "K" (x 10^3)
0.2C mild steel on itself*.	1570	186	0.62	7
60/40 brass	240	95	0.24	60
Teflon	200	5	0.18	250
70/30 brass	100	68	-	17
Perspex	14.5	20	-	7000
Bakelite A	12.0	25	-	7500
Silver steel	7.5	320	-	600
Beryllium copper	7.1	210	-	310
Tool steel	6.0	850	-	13
Stellite	3.2	690	0.60	550
Ferr' stainless steel	2.7	250	0.53	170
Bakelite B	1.8	33	-	1500
Bakelite C	1.0	30	-	75000
Sintered tungsten carbide on mild steel*	0.9	186	-	400
Bakelite D	0.4	29	-	3000
Polythene	0.3	1.7	0.53	13000
Sintered tungsten carbide on itself*.	0.03	1300	0.35	1000

Load 3.9N (0.4 kgf). Sliding speed 1.8m/s.

* Rings are of hardened tool steel except where otherwise stated.

Stated values of hardness are those of the softer materials of the wear couples.

Table 4.1 Unlubricated pin wear rates for various materials with respective values of the coefficient of friction, bulk hardness (of the softer material) and Archard's wear coefficient, K[after Archard and Hirst, 1956 and Archard, 1980].

Classification of wear phenomena according to the type of tribological action

System structure	Tribological action (symbols)	Type of wear	Effective mechanisms (individually or combined)			
			Adhesion	Abrasion	Surface fatigue	Tribo-chemical reactions
Solid – interfacial medium (full fluid film separation) – solid	sliding rolling impact	–			×	×
Solid – solid (with solid friction, boundary, lubrication, mixed lubrication)	sliding	sliding wear	×	×	×	×
	rolling	rolling wear	×	×	×	×
	impact	impact wear	×	×	×	×
	oscillation	fretting wear	×	×	×	×
Solid – solid and particles	sliding	sliding abrasion		×		
	sliding	sliding abrasion (three body abrasion)		×		
	rolling	rolling abrasion (three body abrasion)		×		
Solid – fluid with particles	flow	particle erosion (erosion wear)		×	×	×
Solid – gas with particles	flow	fluid erosion (erosion wear)		×	×	×
	impact	impact particle wear		×	×	×
Solid – fluid	flow oscillation	material cavitation, cavitation erosion			×	×
	impact	drop erosion			×	×

Table 4.2 Classification of wear phenomena according to type of tribological action[from DIN 50 320, 1979].

steel	V.p.n.	sliding speed (cm/s)	T_1 load (Kg)	T_1 θ_m (°C)	T_2 load (Kg)	T_2 θ_m (°C)	T_3 load (Kg)	T_3 θ_m (°C)
0·12 % C	141	20	0·625	70	—	—	—	—
		67	0·150	100	—	—	—	—
		100	0·040	90	18	900	—	—
		133	—	—	9·5	860	—	—
		167	—	—	8·5	950	—	—
		200	—	—	6·5	990	—	—
		266	—	—	4·5	1030	—	—
0·34 % C	205	1·73	2·75	20	—	—	—	—
		33·3	0·5	120	—	—	—	—
		67	0·275	170	—	—	—	—
		100	0·1	160	7·5	850	10	950
		133	0·02	100	5·5	920	—	—
		200	—	—	1·3	750	—	—
0·52 % C	236	1·73	1·75	15	—	—	—	—
		6·7	1·25	50	—	—	—	—
		33	0·6	140	—	—	—	—
		67	0·4	220	20	1030	—	—
		100	0·15	210	5·5	860	7	950
	(A) 212	100	0·15	200	5·5	810	8	920
	236	133	—	—	2·5	810	—	—
		200	—	—	0·125	350	—	—
0·63 % C	260	6·7	3·5	80	—	—	—	—
		100	0·25	260	1·25	310	5·5	900
0·78 % C	278	20	11·75	360	—	—	—	—
		33	9·0	500	—	—	—	—
		47	11·75	720	22·5	920	—	—
		67	—	—	—	—	12	950
		100	—	—	—	—	4·5	900
	(A) 258	100	0·15	200	0·65	400	5	870
	(A) 197	100	—	—	1·6	490	8	870
0·98 % C	319	33	22·5	760	37·5	900	—	—
		47	—	—	—	—	20	940
		100	—	—	—	—	3	830
	(A) 216	100	—	—	1·5	630	5	790

(A), annealed steel.

Table 4.3 Calculated values for maximum hot spot temperatures (θ_m °C above ambient) corresponding to the transitions T_1, T_2 and T_3 [from Welsh, 1965]. (Note - bulk hardness values are given, not wear surface.)

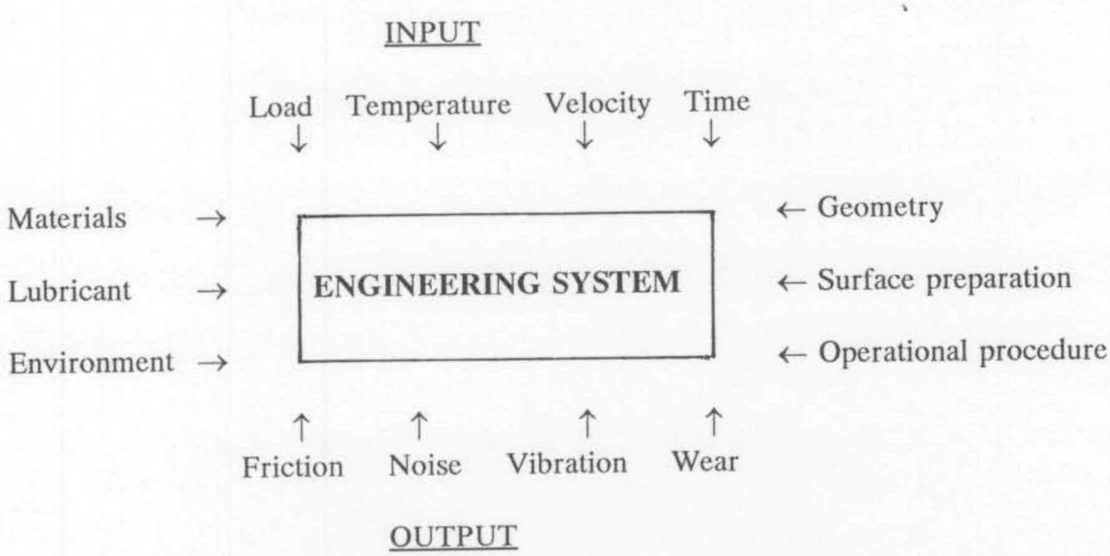

Figure 4.1 The input and output of an engineering system[after Czichos, 1974].

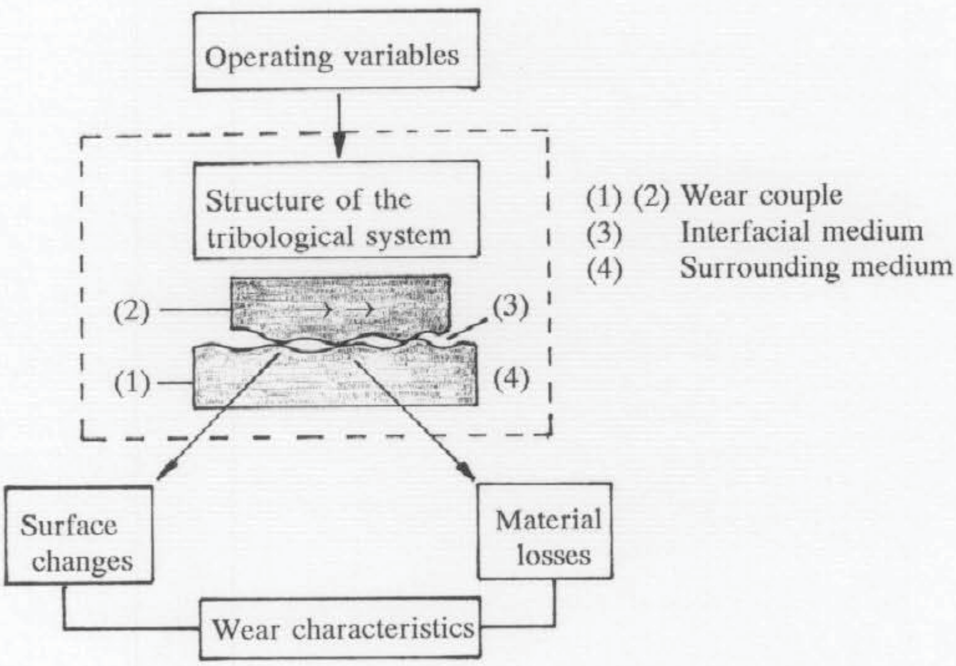

Figure 4.2 A tribological system[after DIN 50 320, 1979].

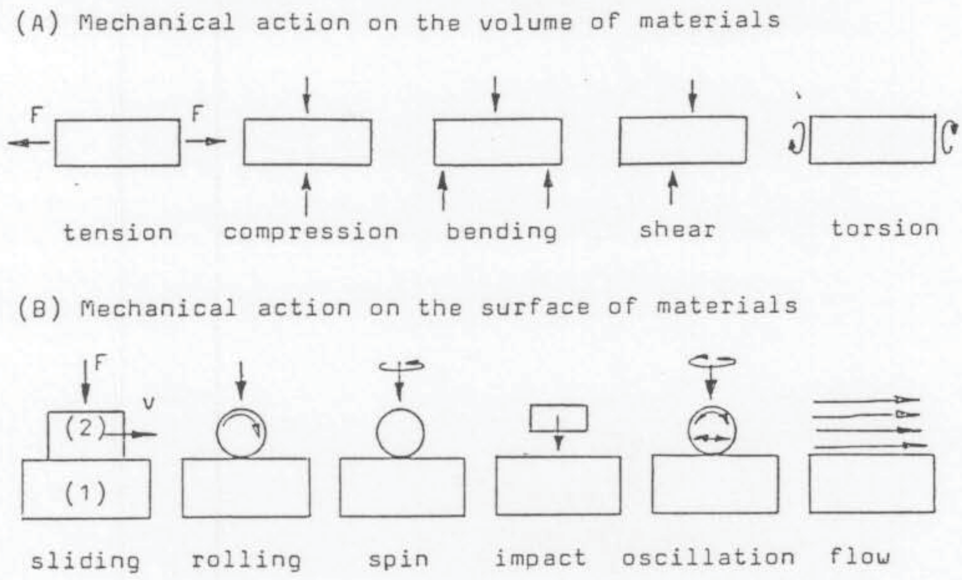

Figure 4.3 A comparison between types of mechanical action on material volumes and material surfaces[from Czichos, 1981].

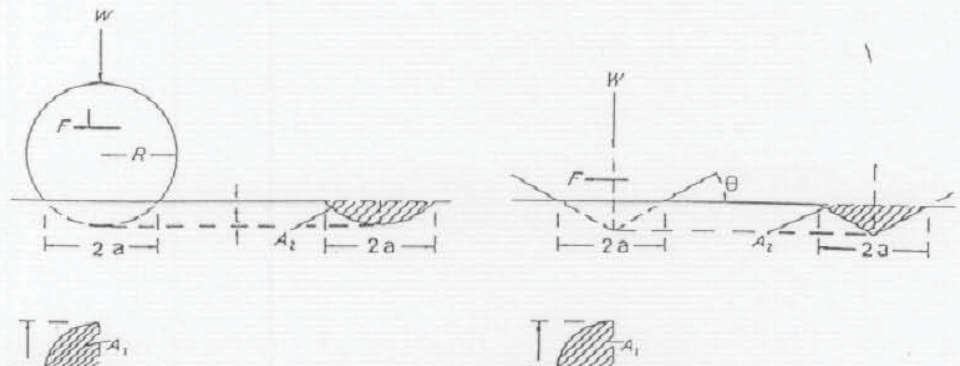

(a) $\mu_p = A_2/A_1 = 4a/3\pi R = 0{\cdot}6\sqrt{t/R}$ (b) $\mu_p = A_2/A_1 = (2/\pi)\tan\theta$

Figure 4.4 Ploughing (or grooving) component of friction, μ_p, for (a) a spherical slider and (b) a conical slider[from Tabor, 1987].

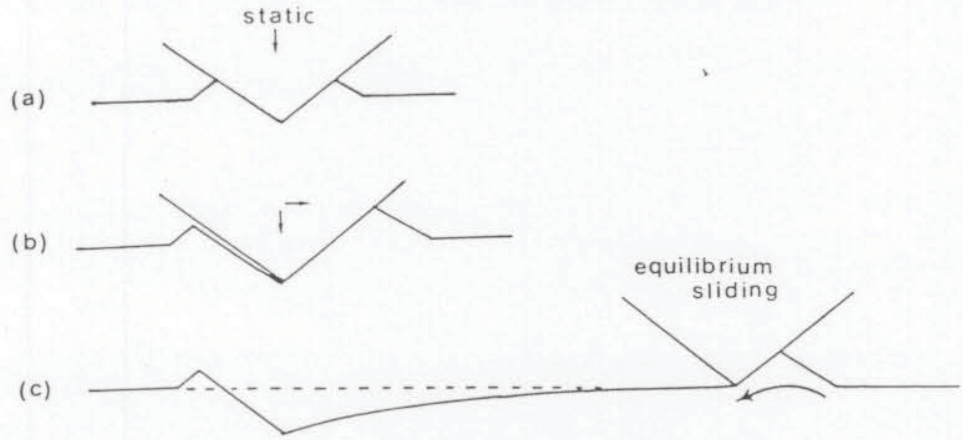

Figure 4.5 A hard two-dimensional wedge on a softer metal surface[from Tabor, 1987]. (a) Static loading. (b) Initial displacement where wedge pushes into surface. (c) Equilibrium conditions after sliding; the wedge has moved back to the original surface level and the prow is continuously ironed into the surface.

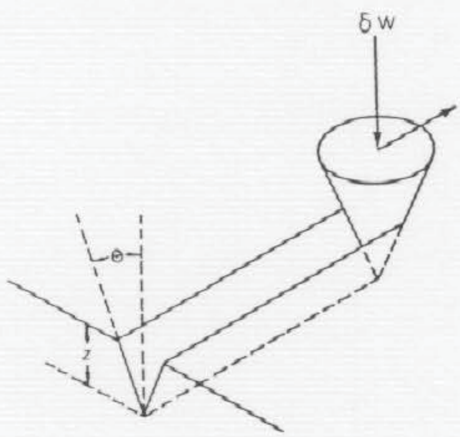

Figure 4.6 Geometric assumptions for Archard's simplified model for abrasive wear[from Archard, 1980].

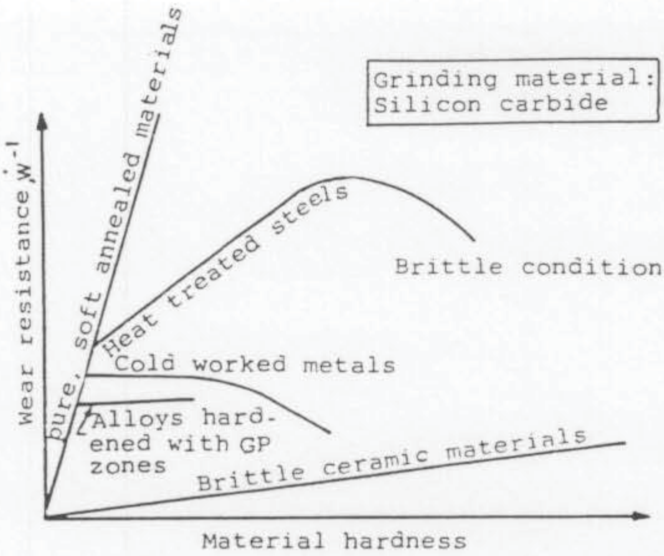

Figure 4.7 The abrasive wear resistance of materials with respect to (wear surface) hardness[Hornbogen, 1981, after Khruschov, 1974].

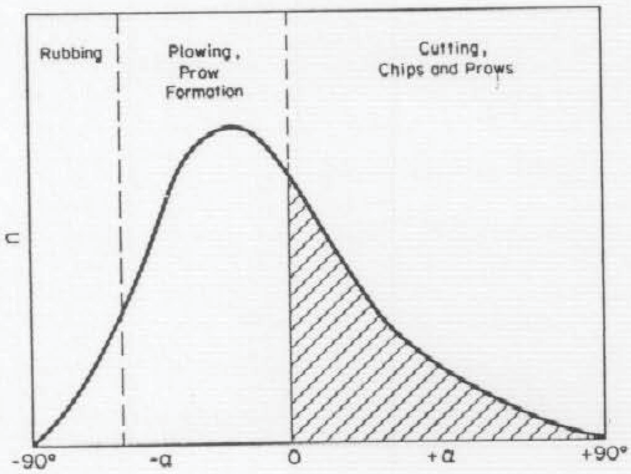

Figure 4.8
A typical distribution of rake angles for abrasive paper and the effect of angle on abrasive wear action[Mulhearns and Samuels, 1962].

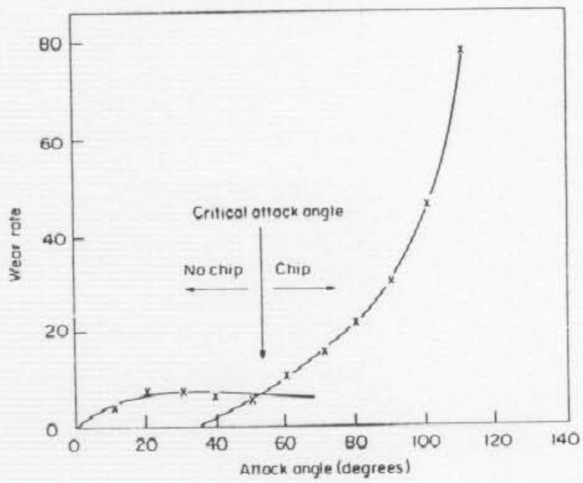

Figure 4.9
Effect of abrasive particle attack angle on wear rate[Eyre, 1979].

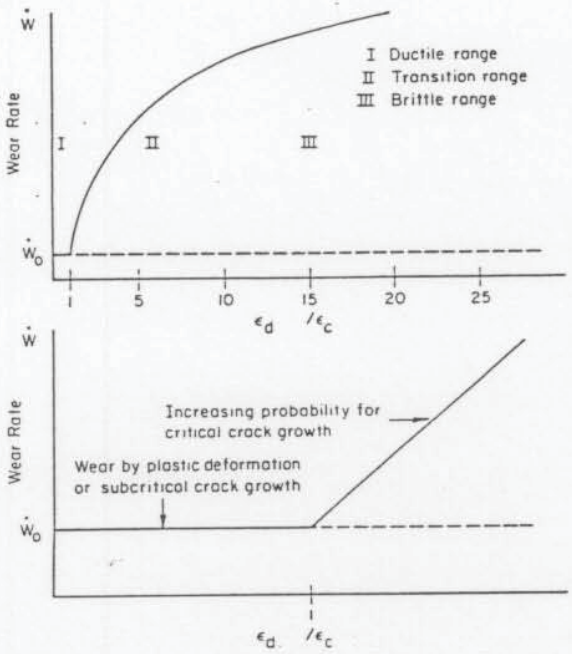

Figure 4.10 Schematic representation for three ranges of abrasive wear behaviour for constant hardness and pressure[from Hornbogen, 1975].

$\varepsilon_d/\varepsilon_c$ - (plastic strain produced during asperity interaction) / (critical strain at which a crack starts to propagate).

Range I - wear rate is independent of high fracture toughness; sub-critical crack growth.

Range II - if critical strain exceeds applied strain then wear rate starts to increase and become dependent on critical crack growth.

Range III - for low toughness, hard brittle materials, a limiting value of maximum wear rate may exist.

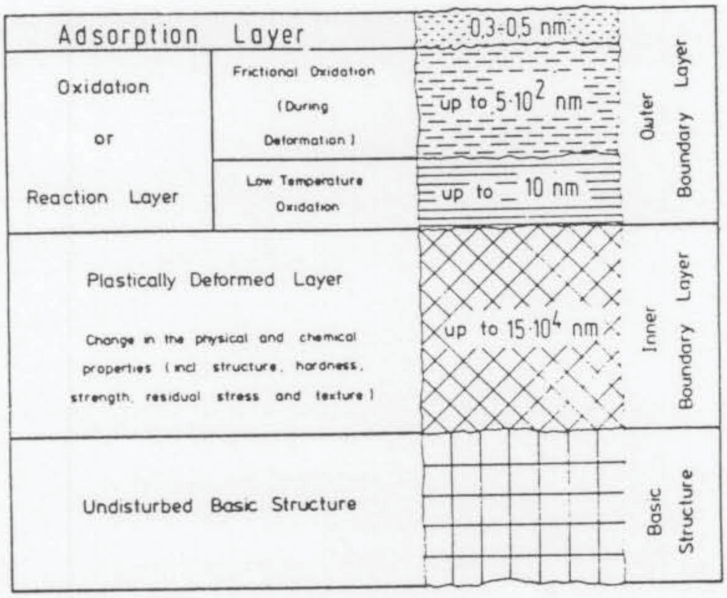

Figure 4.11 Typical composition of surface layers on a metallic wear body[from Krause and Schroelkamp, 1982].

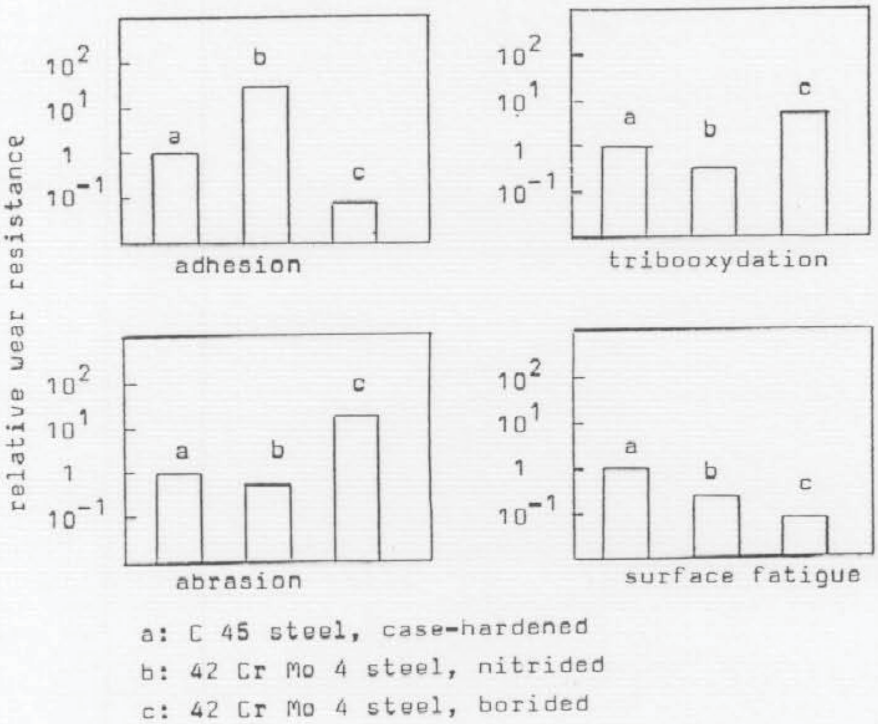

Figure 4.12 Wear resistance ranking of three steel surfaces for different wear mechanisms[from Czichos, 1981].

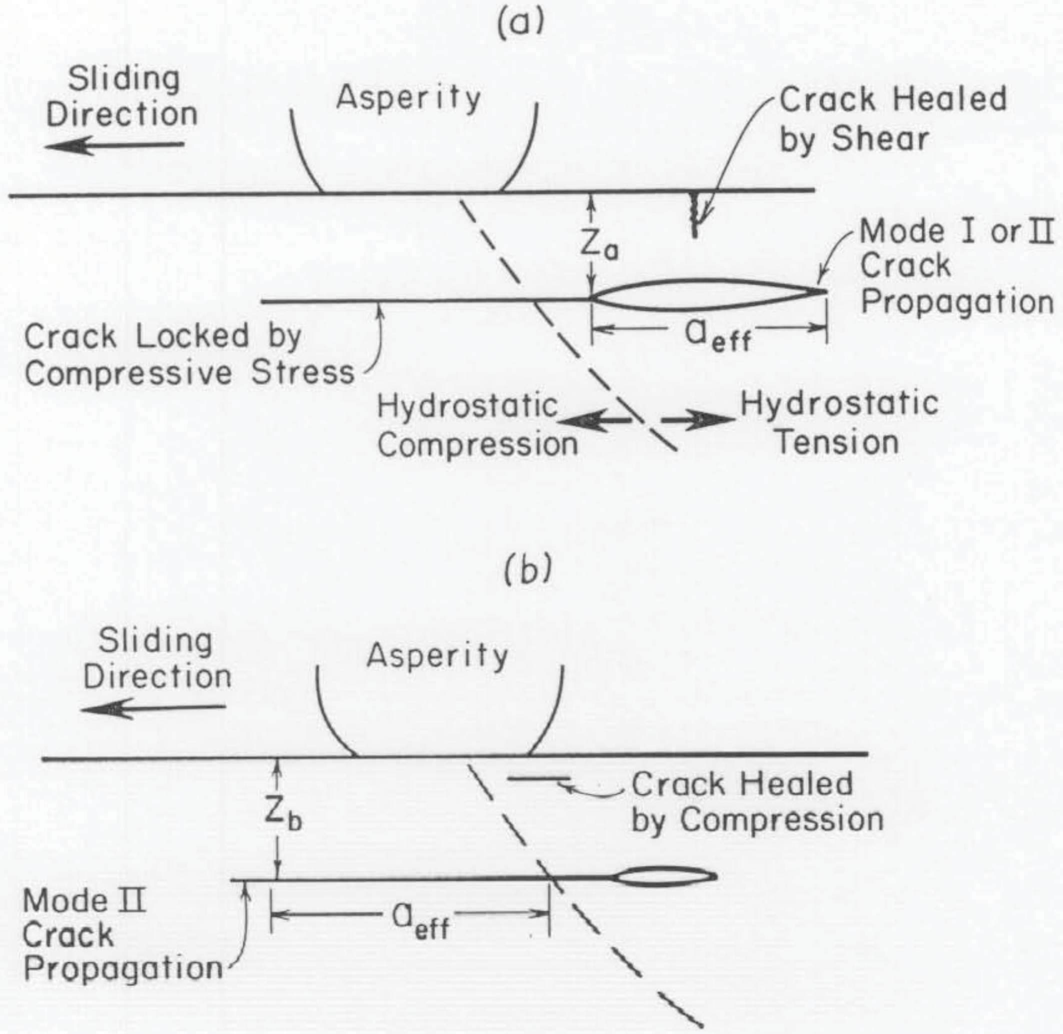

Figure 4.13 Delamination modes[from Hirth and Rigney, 1979].
(a) Model of Suh and coworkers[1977] for mode I or mode II crack propagation parallel to the surface, but at a distance z_a below it, in the region of tensile stress behind the contact. Effective crack length, a_{eff}, is shown.
(b) Hirst and Rigney model for mode II crack propagation.

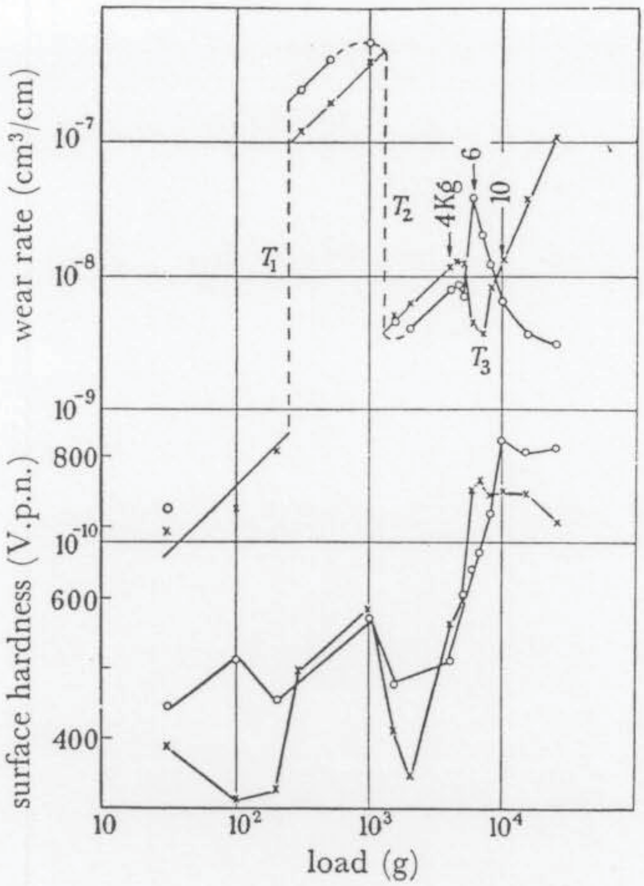

(a)

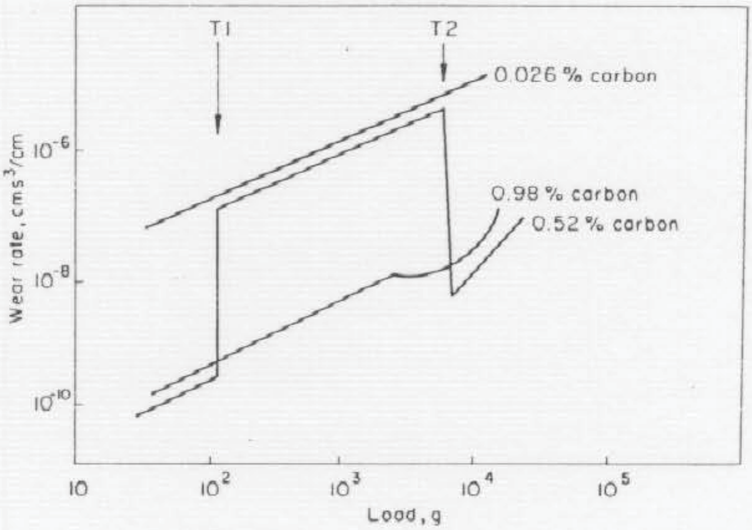

(b)

Figure 4.14 Sharp transitions in sliding wear rate.
(a) Transitions with increases in load and associate hardness changes[from Welsh, 1965]. Sliding speed 100 cm/s, x, pin; o, ring.
(b) Transition wear behaviour of different steels[from Eyre, 1978].

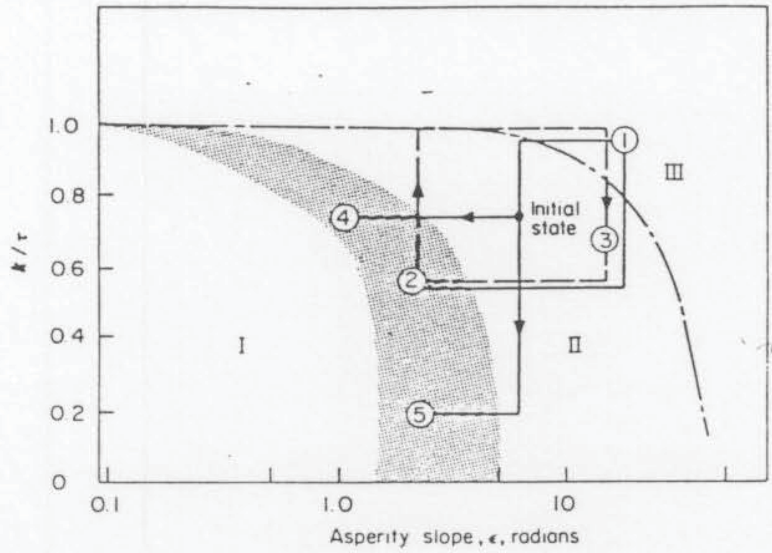

Figure 4.15 Mechanical regimes of sliding wear[from Childs, 1980]. Paths 1 to 5 represent possible changes of surface state caused by sliding.
Path 1 - breakdown of protective surface film.
Path 2 - burnishing to elastic, low wear state.
Path 3 - cyclic removal of run-in layer with renewed adhesive transfer, modification and running-in.
Paths 4 and 5 - protective surface layers prevent adhesive transfer. Running-in is established by burnishing and slow film removal to give elastic, or near elastic conditions, at various stress levels depending upon the nature of the surface films.

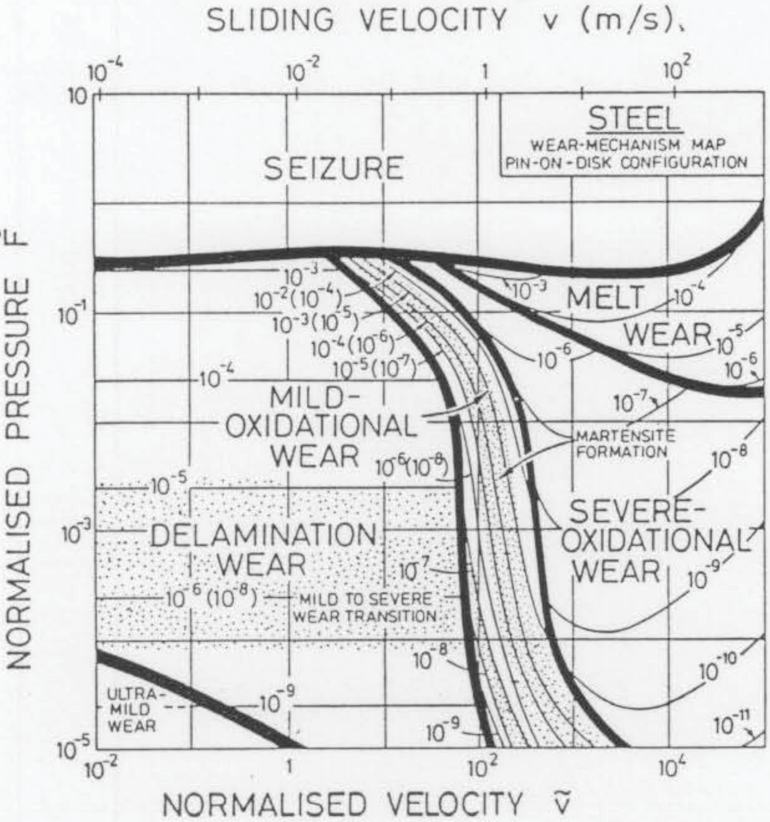

Figure 4.16 Wear mechanism map for a steel pin sliding on a steel disk[from Lim and Ashby, 1987]. Discontinuities in the normalised wear rate contours are where they cross into regimes of severe oxidational and melt wear. Wear rates in parentheses are values when mild wear takes place. Shaded regions indicate mild to severe transitions.

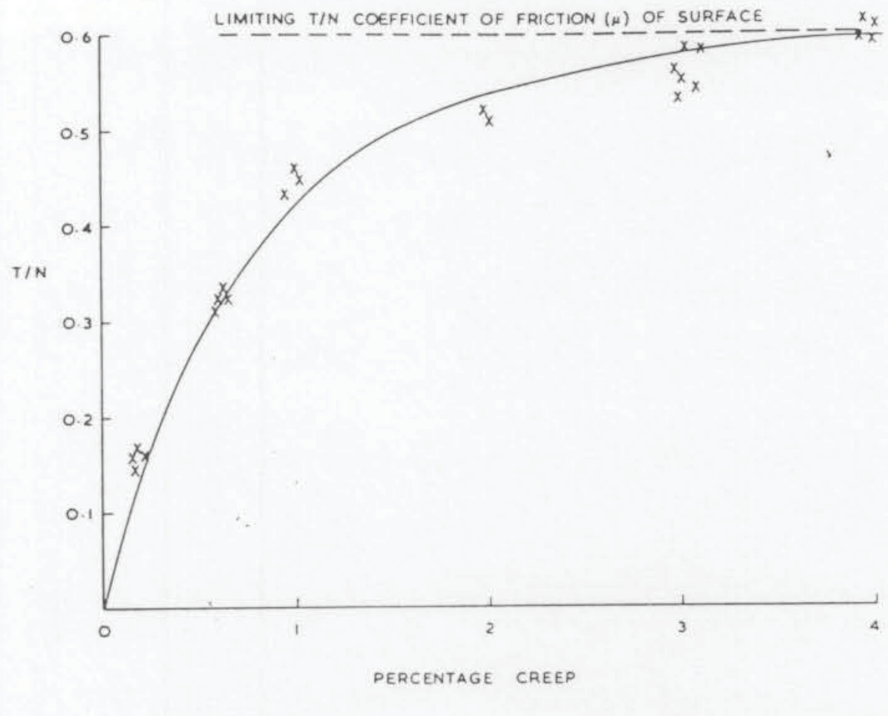

Figure 4.17 Rolling-sliding wear on an Amsler machine; traction coefficient variation with creepage (for uncooled tests with wire brush debris removal)[from Beagley, 1976].

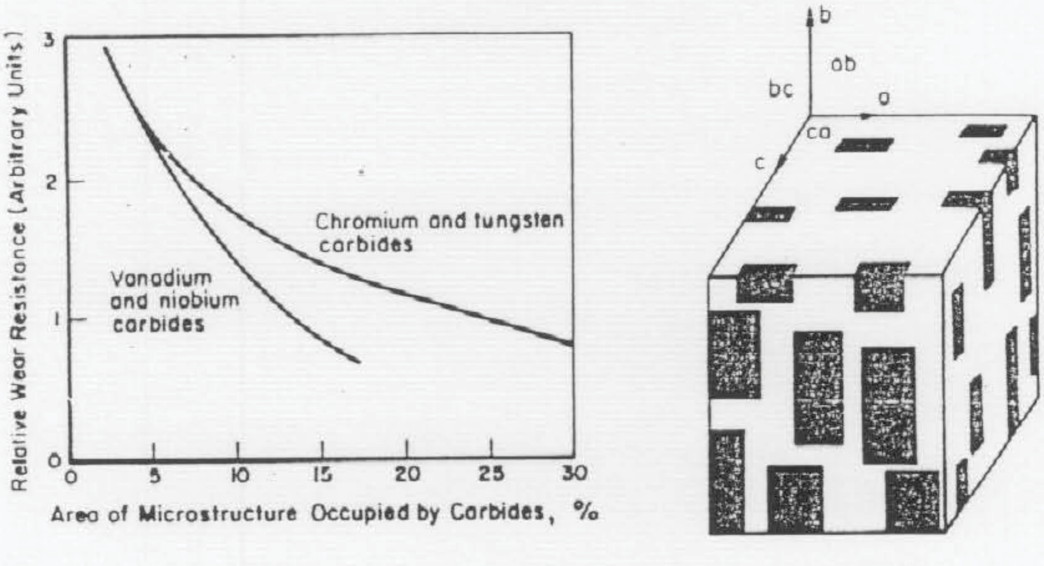

Figure 4.18 The effect of hard second phase particles, their volume fraction, shape and orientation, on wear rate[from Hornbogen, 1981]. (a:b:c - 100:10:1)